physiological conditions. Hypoxia and drugs such as fenfluramine affect the function and expression of K_V (Weir *et al.*, 1996; Patel *et al.*, 1997; Wang *et al.*, 1998; Hulme *et al.*, 1999; Perez-Garcia *et al.*, 2000; Yuan, 2001; Patel & Honore, 2001; Platoshyn *et al.*, 2001). In addition, dysfunction of K_V is known in the PASMCs obtained from patients with primary pulmonary hypertension (Yuan JX *et al.*, 1998).

K_V currents can be divided into two types in smooth muscle cells including PASMCs: delayed rectifier K^+ current (I_K) and transient outward current (I_A). The diversity of subunits underlying K_V allows the formation of channels with different properties (Stuhmer *et al.*, 1998; Coppock & Tamkun, 2001; Davies & Kozlowski, 2001). I_K shows delayed activation and slow inactivation, and is involved in modulating membrane potential and vascular tone in vessels such as the pulmonary artery (PA) (Osipenko *et al.*, 1997; Turner & Kozlowski, 1997; Archer *et al.*, 1998; Gurney *et al.*, 2003). On the other hand, I_A shows rapid activation and inactivation upon depolarization. I_A is not ubiquitous in smooth muscles, but affects membrane excitability, which has been identified in various PASMCs including human (Okabe *et al.*, 1987; Clapp & Gurney, 1991; James *et al.*, 1995; Yuan, 1995; Amberg *et al.*, 2002). Several K_V subunits have been cloned that can form I_A (Baldwin *et al.*, 1991; Pak *et al.*, 1991; Rudy *et al.*, 1991; Schroter *et al.*, 1991; Stuhmer *et al.*, 1998) including $K_V4.1$, $K_V4.2$ and $K_V4.3$ of Shal, $K_V3.3$ and $K_V3.4$ of Shaw and $K_V1.4$ of Shaker. Additionally, K_V1 may form rapidly inactivating K^+ channels when bound to accessory β-subunits (Rettig *et al.*, 1994; Heinemann *et al.*, 1996). By reverse transcriptase–polymerase chain reaction (RT–PCR), Western blotting and immunohistochemistry, both gene and protein expression for various K_V α-subunits have been identified in rat PASMCs (Archer *et al.*, 1998; Yuan XJ *et al.*, 1998; Davies & Kozlowski, 2001; Coppock & Tamkun, 2001; Yuan, 2001). RT–PCR has detected I_A-related genes ($K_V1.4$, $K_V4.1$, $K_V4.2$ and $K_V4.3$) in freshly isolated and primary cultured rat PASMCs (Yuan XJ *et al.*, 1998; Davies & Kozlowski, 2001; Platoshyn *et al.*, 2001; Yuan, 2001), but the molecular and pharmacological diversity of I_A-related K_V α-subunits and K_V channel-interacting protein (KChIP) (An *et al.*, 2000; Bahring *et al.*, 2001), an accessory subunit of K_V4 series, has not been investigated in human PASMCs (hPASMCs).

The present study investigated the molecular and pharmacological characteristics of I_A in cultured hPASMCs, using patch-clamp techniques, RT–PCR, quantitative real-time RT–PCR and immunocytochemical studies.

Methods

Cell preparation

Cultured cells isolated from normal human main pulmonary artery (hPASMCs) were purchased from Clonetics Corporation (San Diego, U.S.A.). The cells used for this study were obtained from six donors. The cells were cultured in 78.5 cm^2 flasks, in culture medium supplemented with 5% fetal calf serum, human epidermal growth factor (0.5 $\mu g\,ml^{-1}$), insulin (5 $mg\,ml^{-1}$), human fibroblast growth factor (1 $\mu g\,ml^{-1}$), gentamicin (50 $\mu g\,ml^{-1}$) and amphotericin B (0.05 $\mu g\,ml^{-1}$) (SmGM-2 Buffer-Kit, Clonetics) in an atmosphere of 5% CO_2 and 95% air at 37°C. At confluence, cells obtained from 78.5 cm^2 flasks were passaged using 0.25–0.5% trypsin in 0.02% EDTA. The medium was replaced twice weekly. Cells just at confluence of passages 3–8 were detached from the culture flasks with 0.25–0.5% trypsin in 0.02% EDTA, and used for later experiments. The cells were identified as smooth muscle cells, by staining α-actin, but not fibroblast growth factor, by immunostaining with biotin-conjugated antibody. All experiments were performed at 35–37°C.

Solutions and agents

The composition of control extracellular Tyrode solution was as follows (in mM): NaCl 136.5, KCl 5.4, $CaCl_2$ 1.8, $MgCl_2$ 0.53, glucose 5.5 and HEPES–NaOH buffer 5.5 (pH 7.4). The patch pipette contained (in mM): KCl 140, EGTA 10, $MgCl_2$ 2, Na_2ATP 3, guanosine-5′-triphosphate (GTP, sodium salt, Sigma) 0.1 and HEPES–KOH buffer 5 (pH 7.2). 4-Aminopyridine (4-AP), tetraethylammonium (TEA), charybdotoxin (CTX), dendrotoxin (DTX) and clofilium were purchased from Sigma (St Louis, MO, U.S.A.). Blood depressing substrate (BDS)-II and phrixotoxin-II were purchased from Alomone Ltd (Jerusalem, Israel). Flecainide was obtained from Eisai Company (Tokyo, Japan).

Recording technique and data analysis

Membrane currents were recorded with glass pipettes under whole-cell clamp conditions (Hamill *et al.*, 1981; Nakajima *et al.*, 1999), using a patch-clamp amplifier (EPC-7, List Electronics, Darmstadt, Germany). The heat-polished patch electrode had a tip resistance of 3–5 MΩ. The series resistance was compensated, and the raw data were subtracted by leakage currents. All data were acquired, stored and analyzed using a Power Macintosh 7100/80 with the PULSE + PULSEFIT software (HEKA Electronic) and Igor PRO (Wave Metrics, Lake Oswego, OR, U.S.A.) as described previously (Terasawa *et al.*, 2002).

The steady-state inactivation of I_A was estimated using the double-pulse protocol. Conditioning voltage pulses (500 ms duration) to various membrane potentials between −80 and +10 mV were applied from a holding potential of −80 mV. At 10 ms after the end of each conditioning pulse, a test pulse to +40 mV (400 ms duration) was applied to activate I_A. The ratio of I_A amplitude with and without conditioning pulses was plotted against each conditioning voltage. The steady-state activation curve was obtained from the conductance (G_K), determined by dividing the peak current amplitude at each membrane potential (V_m) by the driving force for K^+ ($V_m - E_K$), where E_K is the K^+-equilibrium potential. The time course of recovery from inactivation was measured by double-pulse protocols. The first (PI, 400 ms) and the second pulse (PII, 400 ms) with variable interpulse intervals were applied from −80 to +40 mV.

Data were expressed as mean ± s.e.m. Student's *t*-test was used for statistical analysis and $P<0.05$ was considered significant.

RNA extraction and RT–PCR

Total cellular RNA was extracted using Gene Elute™ Mammalian Total RNA Miniprep Kit (Sigma). For RT–PCR, cDNA (complementary DNA) was synthesized from 1 μg of total RNA with RT with random primers (Toyobo,

Osaka) (Oonuma *et al.*, 2002). The reaction mixture was then subjected to PCR amplification with specific forward and reverse oligonucleotide primers for 35 cycles consisting of heat denaturation, annealing and extension. PCR products were size fractionated on 2% agarose gels, and visualized under UV light. Primers were chosen on the basis of the sequences of human K_V1.1-6, K_V2.1-2, K_V3.1-4 and K_V4.1-3 as shown in Table 1. Total RNA from the human fetal brain (Toyobo, Osaka) was used as a positive control.

Real-time quantitative RT–PCR was performed with the use of real-time Taq-Man technology and a sequence detector (ABI PRISM® 7000, Applied Biosystems, Foster City, CA, U.S.A.). Gene-specific primers and Taq-Man probes were used to analyze transcript abundance. The 18S ribosomal RNA level was analyzed as an internal control and used to normalize the values for transcript abundance of K_V α-subunit family genes and KChIPs family genes. We performed six independent experiments.

Immunocytochemistry

Immunocytochemical analysis for the presence of K_V used polyclonal antibodies against K_V3.4. (Alomone Labs, Jerusalem), K_V4.2 (N-15) and K_V4.3 (C-17) (Santa Cruz Biotechnology Inc., CA, U.S.A.). HPASMCs were cultured on Lab-Tek Chamber Slide Glass (Nalge Nunc International, Naperville), fixed with 2% paraformaldehyde for 45 min, rinsed in phosphate-buffered saline (PBS), then blocked in 0.2% Triton X-100 (Sigma), 1% H_2O_2 in PBS. The cells were rinsed in PBS, and incubated in Block Ace (Dainippon Seiyaku, Osaka, Japan) for 30 min at 37°C. The hPASMCs were then incubated with the primary antibodies overnight at 4°C. For control sections, cells were incubated with Block Ace without primary antibody. Cells were then rinsed in PBS, incubated in biotinylated anti-rabbit IgG or anti-goat IgG (Vector Lab. Inc.) for 30 min at room temperature, rinsed in PBS, incubated in VECTASTAIN ABC kit (Vector Lab. Inc., Burlingame) for 20 min at room temperature, and rinsed in PBS. 3,3′-Diaminobenzidine, tetrahydrochloride (DAB, Dojin, Kumamoto) with 0.06% H_2O_2 in PBS was used to form a colored reaction product. Cells were dehydrated, and cover slides were placed on the slides, and viewed using an Olympus BH-2 microscope (Tokyo).

Immunohistochemistry

Immunohistochemical analysis for the presence of voltage-gated K^+ channels used polyclonal antibodies against K_V3.4, K_V4.2 and K_V4.3. Paraffin-embedded human pulmonary artery sections on glass slides (Human Adult Normal Arteriae Pulmonalis Tissue Slide for main PA and Human Adult Normal Urinary & Respiratory System Multi-Tissue Slide for small PA) were purchased from Biochain Institute Inc. (Hayward, CA, U.S.A.). The glass slides were deparaffinized and rehydrated, and the following process was the same as described for immnocytochemistry.

Results

4-AP-sensitive I_A in cultured hPASMCs

Figure 1a shows typical original current traces recorded with 3 mM ATP and 10 mM EGTA. The cells were held at −70 mV,

Table 1 PCR primers used for amplification of voltage-dependent K^+ channel genes

	Size (bp)		*Sequence ('5-'3)*
Kv1.1	352	Sense	ACC GAG ATA GCT GAG CAG GA
		Antisense	CGA TCT TGC CTC CAA TTG TC
Kv1.2	538	Sense	AGA CCA CGA GTG CTG TGA GA
		Antisense	GGA ATA GGT GTG GAA GGT CA
Kv1.3	457	Sense	TTC GGT GTC CCT ACC CTG TA
		Antisense	GGA AAC ATG GGT TGC TAT GG
Kv1.4	506	Sense	GCT TCC CTC ATT GCT CTG AC
		Antisense	AAA CTT CAA CAG GGC CTC CT
Kv1.5	685	Sense	GTG TAA CGT CAA GGC CAA GAG CAA C
		Antisense	AGA CAG AGG CTT GGA GAC ACA GGA A
Kv1.6	590	Sense	CAA TGG TGG TGT GAG TCG AG
		Antisense	AAT CGT CAT CGT CAG CCT CT
Kv2.1	641	Sense	GTC TCT GGG CTT CAC TTT GC
		Antisense	TGT CTT CCA ACT GCT GAA CG
Kv2.2	245	Sense	CTG GAA GTG TGC GAC GAC TA
		Antisense	TCT CGC CTC AGT TCT TCG TT
Kv3.1	198	Sense	CTG GTC TCC ATC ACC ACC TT
		Antisense	GAA GAT GAC ACG CAT GAG GA
Kv3.2	255	Sense	GTA CCC CCA AAC ATG GTC AG
		Antisense	TTG CCC AGA CAT GTG TCA CT
Kv3.3	308	Sense	CCC AGA CAA GGT GGA GTT TC
		Antisense	CAA TGC GCT CAG CGT AGT AA
Kv3.4	346	Sense	AGA GAC AGA GCC CAT CCT GA
		Antisense	CAG GGC CAG GAA GAT GAT AA
Kv4.1	410	Sense	GGC TCT TTG TGT CAG GAA CC
		Antisense	TGC TGA TAA TGG CAG CTA CG
Kv4.2	301	Sense	GCC TTC TTC TGC TTG GAC AC
		Antisense	GCA AGA AGC CCA ATT CTG AG
Kv4.3	359	Sense	ATC TTC ACC GGG GAG TAC CT
		Antisense	GGG ATG CTT GTG AAC TTG CT

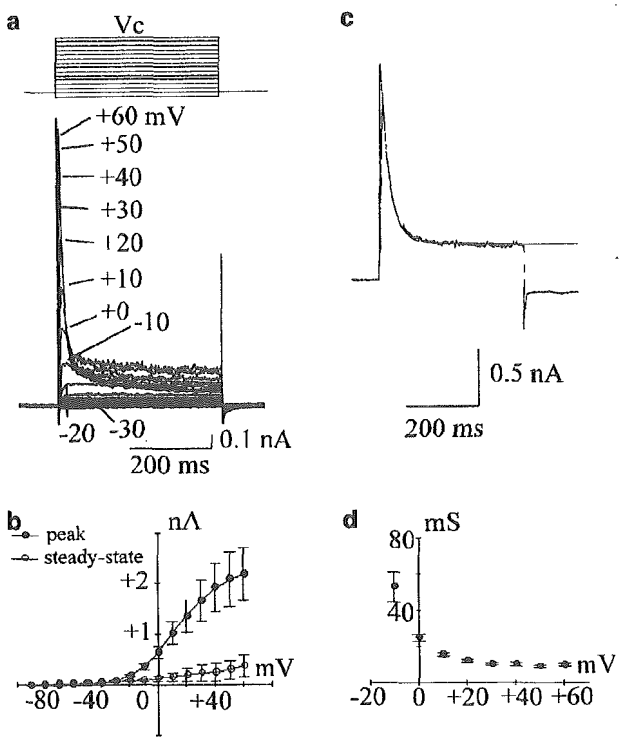

Figure 1 (a) Membrane currents measured with patch pipettes containing 3 mM ATP and 10 mM EGTA. (b) The current–voltage (I–V) relationships measured at the peak (close circles) and steady state (open circles). The data were obtained from six different cells. (c, d) Time courses of inactivation of I_A. The time courses of inactivation of I_A were fitted approximately by single exponential function (c). In (d), the mean±s.e.m. values obtained from three different cells are presented.

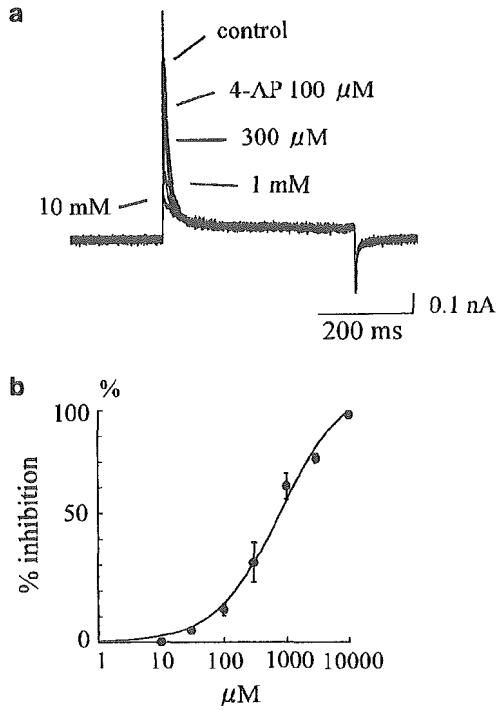

Figure 2 Effects of 4-AP on I_A. (a) Effects of various concentrations of 4-AP. The currents traces are shown in control and in the presence of various concentrations of 4-AP. The cells were held at −80 mV, and command voltage pulses to +40 mV were applied. (b) Concentration-dependent inhibitory effects of 4-AP. Data are shown as mean±s.e.m. (n=3–5), and fit by a Hill equation: % inhibition = $100/\{1+(IC_{50}/[4\text{-AP}])^n\}$, where n represents Hill coefficient, and IC_{50} is 50% inhibitory concentration for 4-AP. The data were best fit with an IC_{50} value of 794 μM and n of 0.8.

and the command voltage pulses to various membrane potentials were applied. During depolarizing pulses, the outward currents with a threshold potential of approximately −40 mV were activated. The currents were rapidly activated, and then rapidly declined to a relatively low steady-state level. Figure 1b shows the current–voltage (I–V) relationships of the outward currents measured at the peak and the steady state. The transient outward current (I_A) and the steady-state outward current (I_K) both increased with depolarization. Figure 1c and d illustrate the time courses of inactivation of I_A. We calculated τ by fitting the I_A decay with a single exponential, and typical data are shown in Figure 1c. The mean±s.e.m. values (n=3) are plotted in Figure 1d against each command potential.

Figure 2 shows the effects of 4-AP on membrane currents. 4-AP inhibited I_A concentration-dependently (Figure 2a), and the half-maximal inhibitory concentration (IC_{50}) was 794 μM (Figure 2b, n=3–5).

RT–PCR and quantitative real-time RT–PCR analysis of K_V α-subunit and KChIP mRNA expression

The above results show the existence of 4-AP-sensitive I_A in cultured hPASMCs. Therefore, we investigated the systematic screening of the expression of K_V genes using RT–PCR (Figure 3). Definite expression of the transcripts of I_A α-subunit-encoding genes (K_V3.4, K_V4.1, K_V4.2 and K_V4.3) as well as I_K-encoding genes (K_V1.1, K_V1.5 and K_V2.1) was observed. However, no definite expression of K_V1.4 and K_V3.3 mRNA was observed. The identity of all K_V homologs seen by RT–PCR was performed by sequencing the relevant band excised from gel to confirm the identity of the product obtained. The quantitative expression of I_A α-subunit-encoding genes (K_V1.4, K_V3.3, K_V3.4, K_V4.1, K_V4.2 and K_V4.3) was investigated by real-time RT–PCR. Transcript levels were normalized to 18S ribosomal housekeeping gene. K_V4.3 appears to be alternatively spliced (Ohya *et al.*, 1997), and the expression of K_V4.3 (long) and K_V4.3 (short) was investigated. As shown in Figure 4a, the relative abundance of the encoding genes of I_A α-subunit was K_V4.2>K_V3.4>K_V4.3 (long)>K_V4.1 with a ratio of 1.00:0.55:0.20:0.09. However, no definite expression of K_V3.3 and K_V4.3 (short) was detected. Thus, it is likely that I_A consists of K_V3.4 and K_V4 currents.

The expression of KChIP, an accessory subunit of K_V4 series, was also investigated by real-time RT–PCR analysis (Figure 4b). KChIP was mainly composed of KChIP3. Neither KChIP1 nor KChIP4 was detected significantly.

Immunocytochemical and immunohistochemical detection of K_V3.4. and K_V4 proteins

Figure 5 shows typical immunocytochemical images obtained from cultured hPASMCs containing I_A in electro-

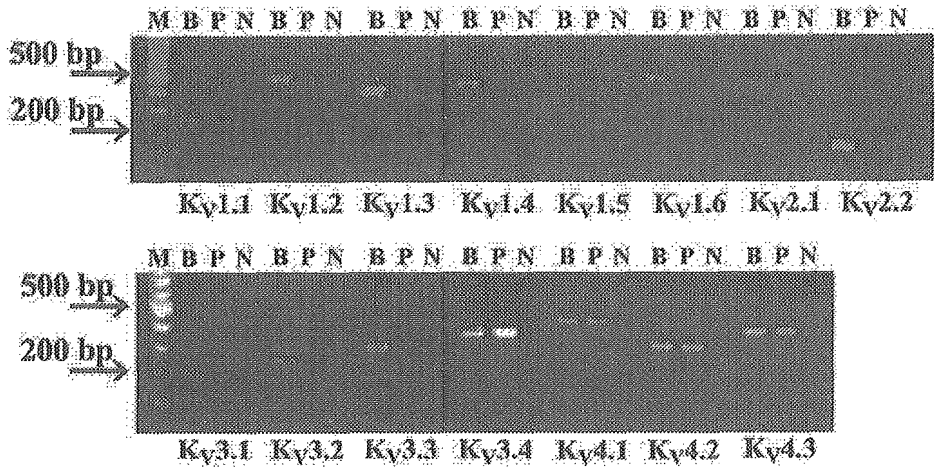

Figure 3 Analysis of K_V mRNA by RT–PCR. Ethidiumbromide-stained gel of RT–PCR products for $K_V1.1$-6, $K_V2.1$-2, $K_V3.1$-4 and $K_V4.1$-3 mRNA. M, marker; N, negative control; B, human brain; P, cultured hPASMCs.

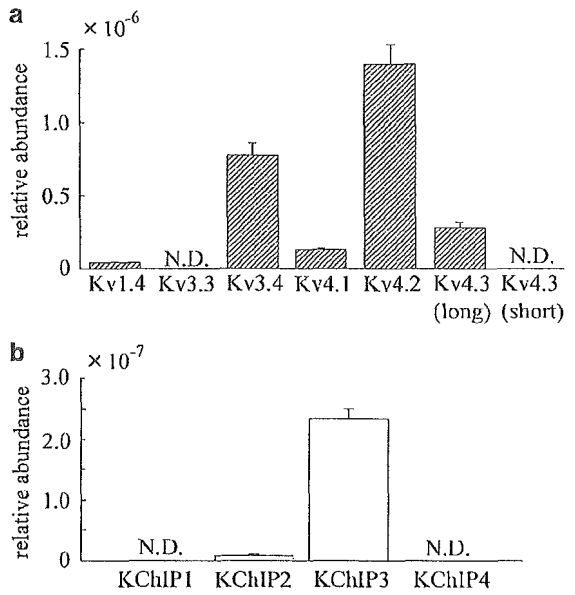

Figure 4 Expression of I_A α-subunit-encoding mRNA (a) and KChIPs mRNA (b) in cultured hPASMCs. The expression levels of I_A α-subunit-encoding genes ($K_V1.4$, $K_V3.3$, $K_V3.4$, $K_V4.1$, $K_V4.2$ and $K_V4.3$ (long and short)) and KChIPs (KChIP1, KChIP2, KChIP3 and KChIP4) genes were normalized to those of the 18S ribosomal RNA levels. Data are means±s.e.m. from six independent samples.

physiological studies. The immunocytochemical studies showed that the cells were immunostained positively with anti-$K_V3.4$ (Figure 5a). Expression of $K_V4.2$ and $K_V4.3$ (Figure 5a) protein was also detected in cultured hPASMCs. Similar results were obtained from three different experiments in each case.

Immunohistochemical studies using hPA sections revealed $K_V3.4$, $K_V4.2$ and $K_V4.3$-like immunoreactivity in intact hPASMCs, as shown in Figures 5b (main PA) and Figure 5c (small PA).

Effects of various K^+ channel blockers on I_A

To investigate the pharmacological characteristics of I_A, the effects of various K^+ channel blockers on I_A were examined. Figure 6A shows the effects of low concentration of TEA (1 mM), which preferentially inhibits $K_V3.4$ compared with K_V4 currents. The cells were held at −80 mV, and command voltage steps to +40 mV were applied. TEA (1 mM) markedly reduced the amplitude of I_A, but higher concentrations of TEA (10 mM) only caused a slight further reduction. The *I–V* relationships measured at the peak and the steady state were plotted in control ($n=6$, Figure 6B, open circle and square) and in the presence of TEA (10 mM, closed circle and square). I_A consisted of a TEA-sensitive component (71.8±6.4% of control I_A in a cell), and a TEA-insensitive component (28.2±6.4%, $n=12$) (Figure 7). Approximately 10% of the cells tested had only TEA-sensitive I_A.

Figures 6C, D and 7 show the effects of BDS-II, a specific blocker of $K_V3.4$ (Diochot *et al.*, 1998), and phrixotoxin-II, a specific blocker of $K_V4.2$ and $K_V4.3$ (Chagot *et al.*, 2004). BDS-II (3 μM) markedly reduced I_A by 67.0±4.7% ($n=3$, Figures 6Ca and 7). It failed to inhibit I_A recorded in the presence of TEA (10 mM, $n=3$, Figure 6Cb) significantly, suggesting that BDS-II selectively inhibited TEA-sensitive I_A in cultured hPASMCs. On the other hand, phyrixotoxin-II (1 μM) reduced it by 36.5±2.0% ($n=3$, Figure 6Da and 7), but it failed to inhibit I_A recorded in a cell containing only TEA-sensitive I_A ($n=3$, Figure 6Db). DTX (100 nM) and CTX (100 nM) inhibited I_A by only 3.0±0.6% ($n=4$) and 1.8±0.6% ($n=4$), respectively (Figure 7). Clofilium (10–50 μM, Figure 7) inhibited I_A by only 2.6±1.1% at 10 μM, and 6.3±1.4% at 50 μM ($n=4$).

The effects of flecainide on I_A are shown in Figure 8. The current traces are shown for the control (Figure 8a) and in the presence of flecainide (10–100 μM, Figure 8a). The *I–V* relationships (Figure 8b, $n=6$) measured at the peak and the steady state are indicated in control and in the presence of flecainide. Flecainde (100 μM) decreased the amplitude of I_A at all command voltages, and inhibited it concentration-dependently. The IC_{50} value of flecainide on control I_A was 113 μM

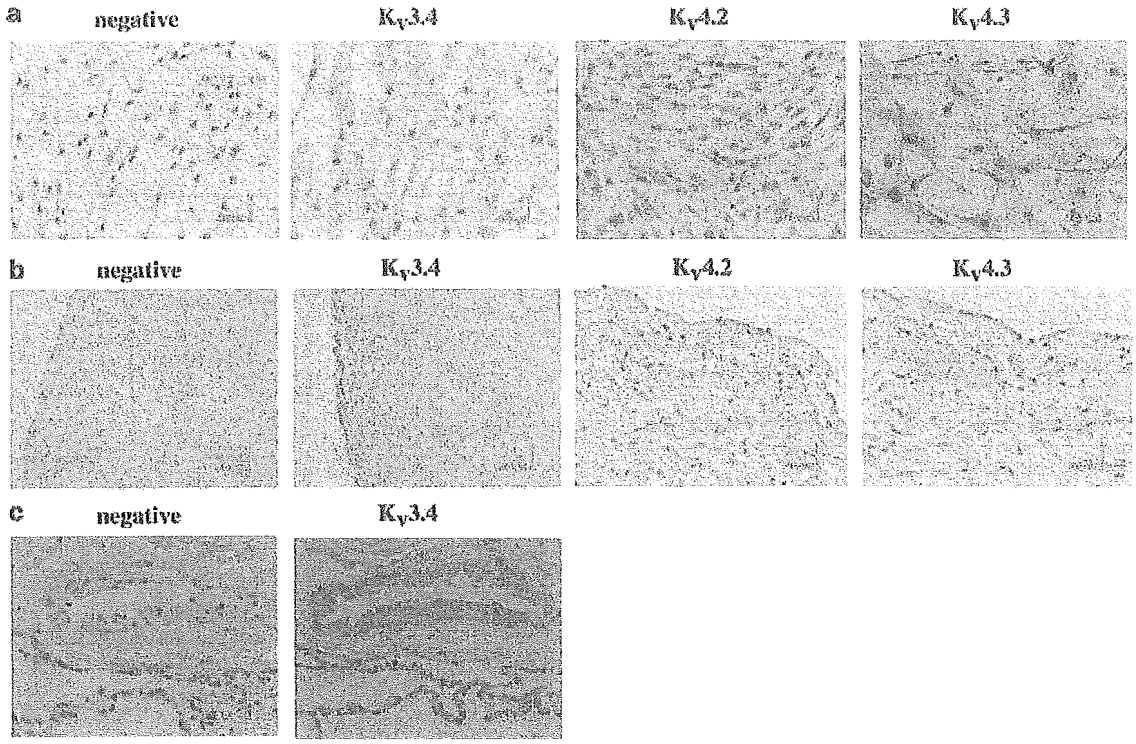

Figure 5 Immunocytochemical and immunohitochemical detection of $K_V3.4$, $K_V4.2$ and $K_V4.3$ protein in cultured hPASMCs (a) and intact human main PA (b) and small PA (c). (a) Expression of $K_V3.4$, $K_V4.2$ and $K_V4.3$ protein in cultured hPASMCs. In the negative control, cells were counterstained with hematoxylin in the absence of anti-$K_V3.4$. (b, c) Immunohistochemical detection of $K_V3.4$, $K_V4.2$ and $K_V4.3$ protein in intact human main PA (b) and small PA (c). Negative controls are shown in each case.

($n=5$). In addition, to compare the effects of flecainide on both TEA-insensitive and TEA-sensitive I_A separately, the effects of flecainide on each component of I_A were examined in a cell containing only TEA-sensitive I_A, and a cell bathed with TEA (10 mM). Flecainide inhibited it with an IC_{50} value of 30 μM in the presence of TEA (10 mM, Figure 8c, $n=4$, closed circles) and with an IC_{50} value of 160 μM in a cell containing only TEA-sensitive I_A (Figure 8c, $n=3$, closed squares).

Kinetics and voltage dependence of two different types of I_A

To clarify the characteristics of the two different types of I_A, the voltage dependence of inactivation of I_A was determined by two-step voltage pulses. Figure 9Aa and Ab show the data from a cell containing only TEA-sensitive I_A, and a cell bathed with TEA (10 mM). The peak amplitude of I_A at each test pulse was normalized to the maximal amplitude of I_A, and the normalized I_A was plotted against the conditioning voltages. The normalized values were fitted to Boltzmann equation using the least-squares methods:

$$I/I_{max} = 1/(1+\exp[(V_m - V_h)/k])$$

where I gives the current amplitude and I_{max} is its maximum, V_m is the potential of the prepulse, V_h is the half-maximal inactivation potential, and k is the slope factor. The TEA-sensitive I_A showed a mean voltage at half inactivation of -23.2 mV, and k of 6.8 ($n=6$, Figure 9Ba), whereas the TEA-insensitive I_A showed values of -54.5 mV, and 7.3 ($n=4$, Figure 9Bb), respectively. The steady-state activation curves were obtained from the conductance as described in Methods, and also fitted to Boltzmann equation (Figure 9B):

$$G_K/G_{K.Max} = 1/(1+\exp[-(V_m - V_h)/k])$$

where $G_{K.Max}$ is the maximal chord conductance, G_K is the chord conductance calculated at the membrane potential (V_m), V_h is the potential at which the conductance is one-half maximally activated and k is the slope factor. The TEA-sensitive I_A showed a mean voltage at half activation of -1.6 mV, and a slope factor of 6.9 ($n=5$, Figure 9Ba), whereas the TEA-insensitive I_A showed values of -2.4 mV and 17.8 ($n=6$, Figure 9Bb), respectively.

The time course of recovery of I_A from inactivation was investigated by the double-pulse protocol (Figure 9C). Figures 9Ca and Cb show the typical data recordings obtained from a cell containing only TEA-sensitive I_A, and a cell bathed with TEA (10 mM). The reactivation time course could be approximately fitted to a single exponential function (Figure 9D). The reactivation time constant was 1521.6 ± 101.4 ms ($n=5$) for the TEA-sensitive I_A, and 238 ± 30 ms ($n=3$) for the TEA-insensitive I_A.

Discussion

The present study showed that I_A in cultured hPASMCs includes two different types of I_A based on the pharmacological and electrophysiological characteristics. Systematic

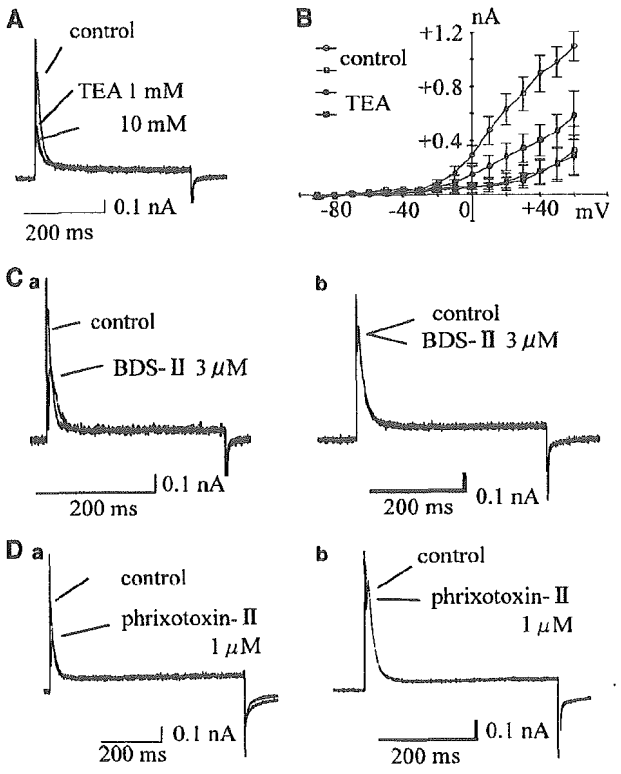

Figure 6 Effects of various K^+ channel blockers on I_A. (A) Effects of TEA (1–10 mM) on I_A. The cells were held at −80 mV, and command voltage pulses to +40 mV were applied at 0.2 Hz. (B) The *I–V* relationships measured at the peak (open and close circles), and the steady state (open and close squares) in control and in the presence of TEA (10 mM). The data are shown as mean ± s.e.m. values ($n = 6$). (C) Effects of BDS-II on I_A recorded in a control cell (a) and in a cell treated with TEA (10 mM, b). (D) Effects of phrixotoxin-II on I_A recorded in a control cell (a) and in a cell containing only TEA-sensitive I_A (b). Each datum is representative of three different cells.

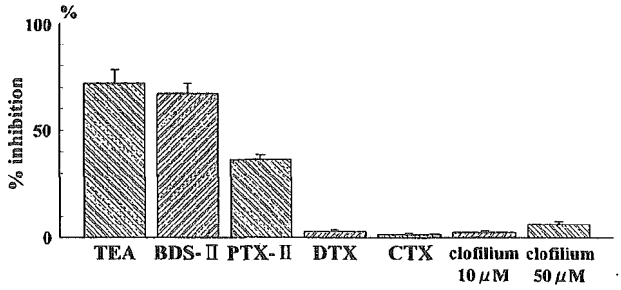

Figure 7 The percent inhibition of various K^+ channel blockers on I_A in cultured human PASMCs. TEA (10 mM, $n = 12$), BDS-II (3 μM, $n = 3$), phrixotoxin-II (PTX-II, 1 μM, $n = 3$), dendrotoxin (DTX, 100 nM, $n = 4$), charybdotoxin (CTX, 100 nM, $n = 4$) and clofilium (10–50 μM, $n = 4$). The cells were held at −80 mV, and command voltage pulses to +40 mV were applied at 0.2 Hz.

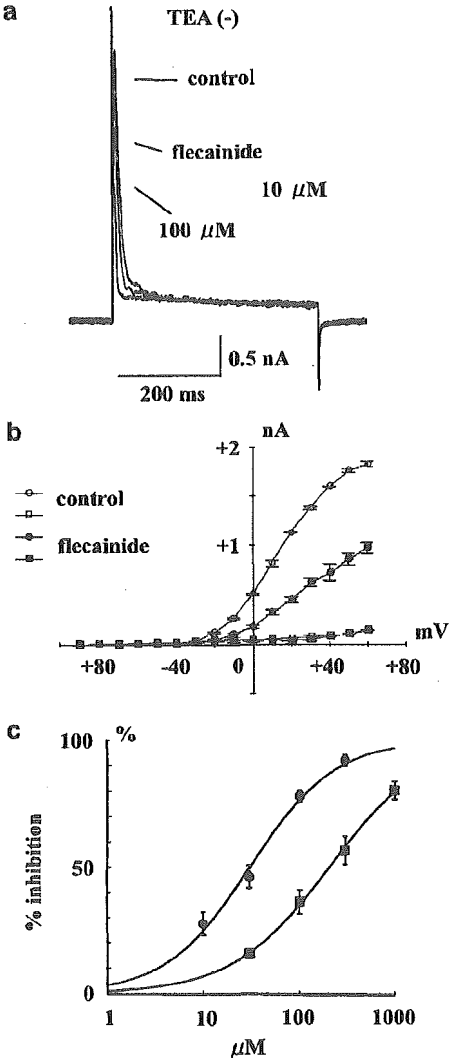

Figure 8 Effects of flecainide on I_A. (a) Effects of flecainide on I_A. The typical current traces are shown in control and after the application of flecainide (10–100 μM). The cells were held at −80 mV, and command voltage pulses to +40 mV were applied. (b) The current–voltage relationships measured at the peak and steady state in control (open circles and squares) and after the application of flecainde (100 μM, closed circles and squares). The data are shown as mean ± s.e.m. values ($n = 6$). (c) Concentration-dependent inhibitory effects of flecainide on I_A recorded in a cell containing only TEA-sensitive I_A (closed squares) and a cell bathed with TEA (10 mM, closed circles). Data are shown as mean ± s.e.m. ($n = 3$), and fitted by a Hill equation: % inhibition $= 100/\{1 + (IC_{50}/[\text{flecainide}])^n\}$, where n represents Hill coefficient, and IC_{50} is 50% inhibitory concentration for flecainide. The data were best fit with an IC_{50} value of 160 μM in a cell containing only TEA-sensitive I_A, and an IC_{50} value of 30 μM in a cell bathed with TEA (10 mM).

screening of the expression of I_A-coding genes using RT–PCR detected the transcripts of the genes encoding for $K_V3.4$, $K_V4.1$, $K_V4.2$ and $K_V4.3$, but not $K_V1.4$ or $K_V3.3$. The detailed quantitative RT–PCR analysis confirmed that the relative abundance of I_A-encoding α-subunit expression was $K_V4.2 > K_V3.4 > K_V4.3$ (long), and KChIP, an accessory subunit of K_V4 series, was mainly composed of KChIP3. The electrophysiological, pharmacological and molecular analyses suggest that I_A in cultured hPASMCs consists of $K_V3.4$ and K_V4 plus KChIP3, which were also confirmed by immunocytochemical studies in cultured hPASMCs and intact PA sections.

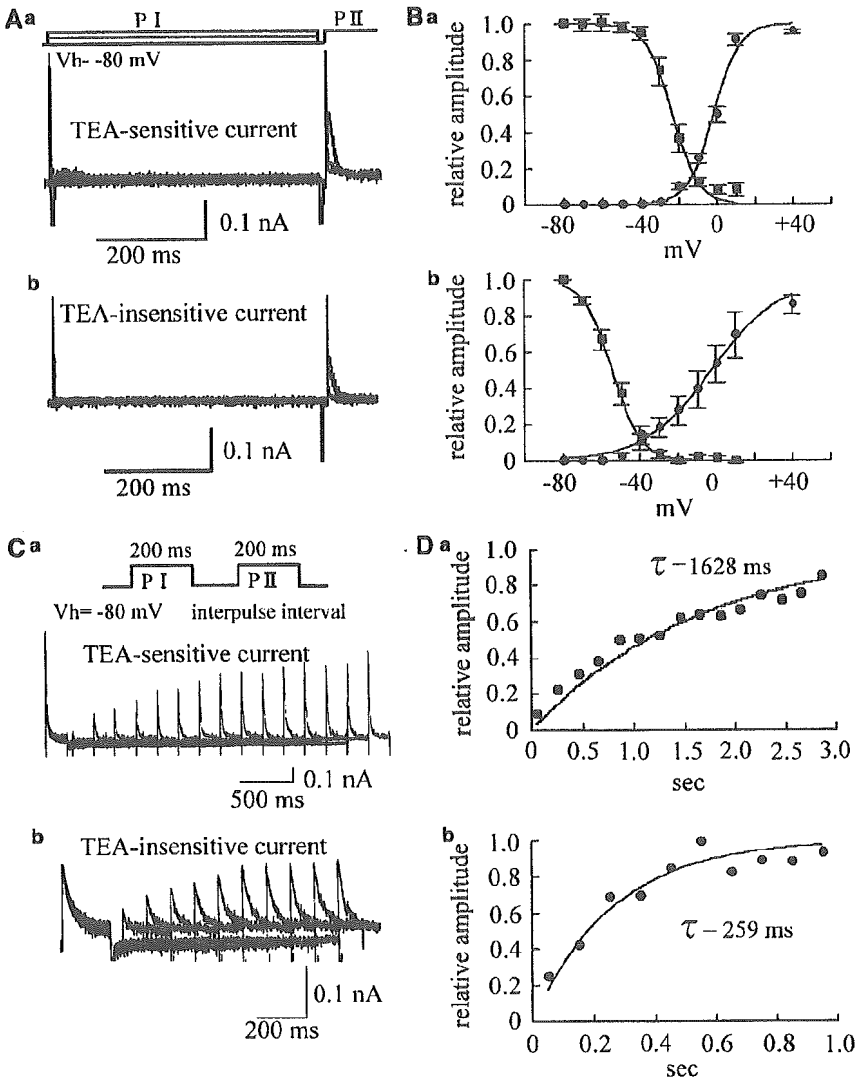

Figure 9 Two components of I_A. (A, B) Steady-state inactivation and activation curves for I_A. Using the double pulse protocol, the steady-state inactivation parameter for I_A was obtained from a cell (Aa), in which only TEA-sensitive current was present, and a cell bathed with TEA (Ab, 10 mM). The typical data were fitted by Boltzmann equation as shown in (B). The steady-state activation curves were also indicated in (B). The mean ± s.e.m. values obtained from four to six different cells. (C, D) Recovery from inactivation of I_A. The data in (C) were obtained from a cell (Ca), where only TEA-sensitive current was present and a cell (Cb) bathed with TEA (10 mM). The fitted data are shown in (D). Each datum is representative of three to five different experiments.

K_V is involved in membrane excitability, and regulates $[Ca^{2+}]_i$ and vascular tone (Nelson & Quayle, 1995). 4-AP, a K_V channel blocker, caused depolarization of the membrane and increased $[Ca^{2+}]_i$ in cultured hPASMCs (data not shown) as found in several types of PASMCs including rat (Yuan, 1995; Weir *et al.*, 1996; Archer *et al.*, 1998). Molecular and electrophysiological studies have shown that I_K-encoding genes such as $K_V2.1$, which are oxygen-sensitive K_V, are involved in hypoxic vasoconstriction of rat PASMCs (Osipenko *et al.*, 1997; Turner & Kozlowski, 1997; Archer *et al.*, 1998; Patel & Honore, 2001; Gurney *et al.*, 2003). Our RT–PCR analysis also detected the I_K-encoding genes ($K_V1.5$ and $K_V2.1$) in cultured hPASMCs. However, in physiological studies, depolarizing pulses elicited I_A, followed by relatively small steady-state K^+ currents (I_K), as reported previously in cultured hPASMCs (James *et al.*, 1995). Therefore, the density of I_K appears to decrease during repetitive subculture as described in rat PASMCs (Yuan *et al.*, 1993). However, the small I_K facilitated the detailed discrimination and investigation of I_A in the present study.

The present study demonstrated the presence of two different types of I_A. 4-AP inhibited I_A with an IC_{50} value of 794 μM, and I_A could be divided into two different components by the sensitivity to TEA. One component was sensitive to low concentrations of TEA. These pharmacological properties were similar to the cloned $K_V3.4$ channel (Rudy *et al.*, 1991; Schroter *et al.*, 1991). Additionally BDS-II, a specific blocker of $K_V3.4$ (Diochot *et al.*, 1998), inhibited I_A, which also supports the existence of $K_V3.4$ channel. The other component of I_A was resistant to these agents, and inhibited by phrixotoxin-II, a selective blocker of $K_V4.2$ and $K_V4.3$ (Chagot *et al.*, 2004), suggesting that this component consists of K_V4

currents. In addition, flecainide inhibited I_A, but it preferentially inhibited TEA-insensitive I_A with an IC_{50} of 30 M in comparison with TEA-sensitive I_A. I_A formed by K_V4 currents has been reported to be more sensitive to inhibition by flecainide ($IC_{50}<20\,\mu M$) (Yamashita *et al.*, 1995; Yeola & Snyders, 1997), suggesting that $K_V3.4$ current is resistant to flecainide compared with K_V4 currents, and I_A in cultured hPASMCs is composed of these two different types of channels.

Two components of I_A could also be distinguished by the kinetic properties of the channels (voltage of half inactivation and time courses of recovery from inactivation). Based on the expression system of $K_V3.4$ and K_V4 ($K_V4.1$, $K_V4.2$, $K_V4.3$) (Pak *et al.*, 1991; Schroter *et al.*, 1991; Coetzee *et al.*, 1999), $K_V3.4$ and K_V4 have the mean voltages at half inactivation of -20 to -32 mV and -50 to 69 mV, and K_V4 shows the fast recovery from inactivation compared with $K_V3.4$, which are consistent with our proposal that I_A consists of two different types of I_A, $K_V3.4$ and K_V4.

RT–PCR analysis identified the I_A-related genes (Baldwin *et al.*, 1991; Pak *et al.*, 1991; Rudy *et al.*, 1991; Schroter *et al.*, 1991) encoding for $K_V3.4$, $K_V4.1$, $K_V4.2$ and $K_V4.3$, but not $K_V1.4$ or $K_V3.3$, irrespective of passage numbers (3 and 8). The detailed quantitative real-time RT–PCR analysis provided evidence that the relative abundance of I_A-encoding α-subunit expression was $K_V4.2>K_V3.4>K_V4.3$ (long)$>K_V4.1$ with a ratio of 1.00 : 0.55 : 0.20 : 0.09. K_V1 coexpressed with accessory β-subunits can also form I_A (Rettig *et al.*, 1994; Heinemann *et al.*, 1996). However, DTX, a blocker of $K_V1.1$ and $K_V1.2$, CTX, a blocker of $K_V1.2$ and $K_V1.3$ (Grissmer *et al.*, 1994) and clofilium, a blocker of $K_V1.5$ (Malayev *et al.*, 1995), did not inhibit I_A. Therefore, the channel of K_V1 does not seem to be involved in forming I_A in hPASMCs. These observations suggest that I_A consists of two different types of I_A, $K_V3.4$ and K_V4. RT–PCR has shown the presence of $K_V3.4$, $K_V4.1$, $K_V4.2$ and $K_V4.3$ mRNA in rat PASMCs (Yuan XJ *et al.*, 1998; Davies & Kozlowski, 2001; Platoshyn *et al.*, 2001; Yuan, 2001), but the present study provided the direct evidence in cultured hPASMCs based on electrophysiological and molecular analyses. The immunocytochemical findings of $K_V3.4$ corresponded well with the results of RT–PCR. The presence of $K_V3.4$ was also confirmed by the immunohistochemical studies using intact hPA sections of the main and small PA. RT–PCR also showed the presence of $K_V4.1$, $K_V4.2$ and $K_V4.3$ mRNA, and the real-time RT–PCR analysis clearly provided the evidence showing that the relative abundance of K_V was $K_V4.2>K_V4.3$ (long)$>K_V4.1$. In this study, we showed that transcripts encoding $K_V4.2$ and $K_V4.3$ were 11- and two-fold more abundant than $K_V4.1$ transcripts, respectively. The immunocytochemical findings also showed that $K_V4.2$ and $K_V4.3$ were expressed in cultured hPASMCs, and in intact hPA sections. We could not rule out the possible involvement of $K_V4.1$ on I_A, because anti-$K_V4.1$ antibody was not commercially available. Further studies are needed to clarify this possibility, but K_V4 is likely to be the major component of TEA-insensitive I_A in cultured hPASMCs. KChIPs, which interact with the NH_2 terminus of K_V4 proteins, enhance surface expression and modulate the kinetics of the channels (An *et al.*, 2000, Bahring *et al.*, 2001). It has been reported that KChIP1 is predominant in murine colonic myocytes (Amberg *et al.*, 2002) and KChIP1 and KChIP3 are extensively expressed in mouse gastrointestinal myocytes (Ohya & Horowitz, 2002). The present study showed that KChIP expressed in cultured hPASMCs is mainly composed of KChIP3. From these observations, we conclude that K_V4, in association with KChIP3, is the major molecular determinant of I_A in cultured hPASMCs.

The functions of I_A in hPASMCs remain unsettled. Both components of I_A (K_V4 and $K_V3.4$ currents) were activated at potentials more positive than -40 mV, which suggests that it may not play an important role in forming membrane potential in hPASMCs. Instead, it is likely that I_A inhibits membrane excitability and prevents depolarizing stimuli such as hypoxia under the pathophysiological conditions (Osipenko *et al.*, 1997; Turner & Kozlowski, 1997; Archer *et al.*, 1998; Patel & Honore, 2001; Gurney *et al.*, 2003). In addition, $K_V3.4$ appears to be modulated by oxidant stress (Serodio *et al.*, 1994; Duprat *et al.*, 1995), proposing that $K_V3.4$ may play a modulatory role in excitability of hPASMCs under the various pathophysiological conditions such as hypoxia. However, further studies are needed to clarify the physiological significance of I_A in hPASMCs.

In conclusion, I_A in cultured hPASMCs consists of two kinetically and pharmacologically distinct components, possibly $K_V3.4$ and K_V4 plus KChIP3.

Limitations of our study

The present study used cultured hPASMCs instead of freshly isolated cells because it is difficult for us to obtain human tissues. The presence of a heterogeneous population of smooth muscle cells in the PA has been reported (Smirnov *et al.*, 2002), but expression of $K_V3.4$ and K_V4 was detected in cultured hPASMCs irrespective of passage number, and was confirmed by immunohistochemical analysis using PA preparations. Therefore, the findings obtained from the present study are likely to hold in native human PA, but further studies using freshly isolated hPASMCs are needed.

References

AMBERG, G.C., KOH, S.D., IMAIZUMI, Y., OHYA, S. & SANDERS, K.M. (2002). A-type potassium currents in smooth muscle. *Am. J. Physiol.*, **284**, C583–C595.

AN, W.F., BOWLBY, M.R., BETTY, M., CAO, J., LING, H.P., MENDOZA, G., HINSON, J.W., MATTSON, K.I., STRASSLE, B.W., TRIMMER, J.S. & RHODES, K.J. (2000). Modulation of A-type potassium channels by a family of calcium sensors. *Nature*, **403**, 553–556.

ARCHER, S.L., SOUIL, E., DINH-XUAN, A.T., SCHREMMER, B., MERCIER, J.C., YAAGOUBI, A., NGUYEN-HUU, L., REEVE, H.L. & HAMPL, V. (1998). Molecular identification of the role of voltage-gated K^+ channels, $K_V1.5$ and $K_V2.1$ in hypoxic pulmonary vasoconstriction and control of resting membrane potential in rat pulmonary artery myocytes. *J. Clin. Invest.*, **101**, 2319–2330.

BAHRING, R., DANNENGERG, J., PETERS, H.C., LEICHER, T., PONGS, O. & ISBRANDT, D. (2001). Conserved K_V4 N-terminal domain critical for effects of K_V channel-interacting protein 2.2 on channel expression and gating. *J. Biol.Chem.*, **276**, 23888–23894.

BALDWIN, T.J., TSAUR, M.L., LOPEZ, G.A., JAN, Y.N. & JAN, L.Y. (1991). Characterization of a mammalian cDNA from an inactivating voltage-sensitive K^+ channel. *Neuron*, **7**, 471–483.

CHAGOT, B., ESCOUBAS, P., VILLEGAS, E., BERNARD, C., FERRAT, G., CORZO, G., LAZDUNSKI, M. & DARBAN, H. (2004). Solution structure of Phrixotoxin-1, a specific peptide inhibitor of K_V4 potassium channels from the venom of the theraphoid spider *Phrixotrichus auratus*. *Protein Sci.*, **13**, 1197–1208.

CLAPP, L.H. & GURNEY, A.M. (1991). Outward currents in rabbit pulmonary artery cells dissociated with a new technique. *Exp. Physiol.*, **76**, 677–693.

COETZEE, W.A., AMARILLO, Y., CHIU, J., CHOW, A., LAU, D., MECORMACK, T., MORENO, H., NADAL, M.C., OZAITA, A., POUNTNEY, D., SAGANICH, M., VEGA-SAENY DE MIERA, E. & RUDY, B. (1999). Molecular diversity of K^+ channels. *Ann. N. Acad. Sci.*, **868**, 233–285.

COPPOCK, E.A. & TAMKUN, M.M. (2001). Differential expression of K(V) channel alpha- and beta-subunits in the bovine pulmonary arterial circulation. *Am. J. Physiol.*, **281**, L1350–L1360.

DAVIES, A.R. & KOZLOWSKI, R.Z. (2001). Kv channel subunit expression in rat pulmonary arteries. *Lung*, **179**, 147–161.

DIOCHOT, S., SCHWEITZ, H., BERESS, L. & LAZDUNSKI, M. (1998). Sea anemone peptides with a specific blocking activity against the fast inactivating potassium channel $K_V3.4$. *J. Biol. Chem.*, **273**, 6744–6749.

DUPRAT, F., GUILLEMARE, E., ROMEY, G., FINK, M., LESAGE F LAZDUNSKI, M. & HONORE, E. (1995). Susceptibility of cloned K^+ channels to reactive oxygen species. *Proc. Natl. Acad. Sci. U.S.A.*, **92**, 11796–11800.

GRISSMER, S., NGUYEN, A.N., AIYAR, J., HANSON, D.C., MATHER, R.J., GUTMAN, G.A., KARMILOWICZ, M.J., AUPERIN, D.P. & CHANDY, K.G. (1994). Pharmacological characterization of five cloned voltage-gated K^+ channels, types $K_V1.1$, 1.2, 1.3, 1.5, and 3.1, stably expressed in mammalian cell lines. *Mol. Pharmacol.*, **45**, 1227–1234.

GURNEY, A.M., OSIENKO, O.N., MACMILLIAN, D., MCFARLANE, K.M., TATE, R.J. & KEMPSILL, F.E.J. (2003). Two-pore domain K channel, TASK-1, in pulmonary artery smooth muscle cells. *Circ. Res.*, **93**, 957–964.

HAMILL, O.P., MARTY, A., NEHER, E., SAKMANN, B. & SIGWORTH, F.J. (1981). Improved patch-clamp techniques for high-resolution current recording from cells and cell-free membrane patches. *Pflug. Arch.*, **391**, 85–100.

HEINEMANN, S.H., RETTIG, J., GRAACK, H.R. & PONGS, O. (1996). Functional characterization of K_V channel β-subunits from rat brain. *J. Physiol.*, **493**, 625–633.

HULME, J.T., COPPOCK, E.A., FELIPE, A., MARTENS, J.R. & TAMKUM, M.M. (1999). Oxygen sensitivity of cloned voltage-gated K^+ channels expressed in the pulmonary vasculature. *Circ. Res.*, **85**, 489–497.

JAMES, A.F., OKADA, T. & HORIE, M. (1995). A fast transient outward current in cultured cells from human pulmonary artery smooth muscle. *Am. J. Physiol.*, **268**, H2358–H2365.

MALAYEV, A.A., NELSON, D.J. & PHILIPSON, L.H. (1995). Mechanism of clofilium block of the human $K_V1.5$ delayed rectifier potassium channel. *Mol. Pharmacol.*, **47**, 198–205.

NAKAJIMA, T., IWASAWA, K., OONUMA, H., IMUTA, H., HAZAMA, H., ASANO, M., MORITA, T., NAKAMURA, F., SUZUKI, J., SUZUKI, S., KAWAKAMI, Y., OMATA, M. & OKUDA, Y. (1999). Troglitazone inhibits voltage-dependent calcium currents in guinea pig cardiac myocytes. *Circulation*, **99**, 2942–2950.

NELSON, M.T. & QUAYLE, J.M. (1995). Physiological roles and properties of potassium channels in arterial smooth muscle. *Am. J. Physiol.*, **268**, C799–C822.

OHYA, S. & HOROWITZ, B. (2002). Differential transcriptional expression of Ca^{2+} BP superfamilies in murine gastrointestinal smooth muscles. *Am. J. Physiol.*, **283**, G1290–G1297.

OHYA, S., TANAKA, M., OKU, T., ASAI, Y., WATANABE, M., GILES, W.R. & IMAIZUMI, Y. (1997). Molecular cloning and tissue distribution of an alternatively spliced variant of an A-type K^+ channel α-subunit, $K_V4.3$ in the rat. *FEBS Lett.*, **420**, 47–53.

OKABE, K., KITAMURA, K. & KURIYAMA, H. (1987). Features of 4-aminopyridine sensitive outward current observed in single smooth muscle cells from the rabbit pulmonary artery. *Pflugers Arch.*, **409**, 561–568.

OONUMA, H., IWASAWA, K., IIDA, H., NAGATA, T., IMUTA, H., MORITA, Y., YAMAMOTO, K., NAGAI, R., OMATA, M. & NAKAJIMA, T. (2002). Inward rectifier K^+ current in human bronchial smooth muscle cells: inhibition with antisense oligonucleotides targeted to Kir2.1 mRNA. *Am. J. Resp. Cell. Mol. Biol.*, **26**, 371–379.

OSIPENKO, O.N., EVANS, A.M. & GURNEY, A.M. (1997). Regulation of the resting potential of rabbit pulmonary artery myocytes by a low threshold, O_2-sensing potassium current. *Br. J. Pharmacol.*, **120**, 1461–1470.

PAK, M.D., BAKER, K., COVARRUBIAS, M., BUTLER, A., RATCLIFFE, A. & SALKOFF, L. (1991). mShal, a subfamily of A-type K^+ channel cloned from mammalian brain. *Proc. Natl. Acad. Sci. U.S.A.*, **88**, 4386–4390.

PATEL, A.J. & HONORE, E. (2001). Molecular physiology of oxgen-sensitive potassium channels. *Eur. Respir. J.*, **18**, 221–227.

PATEL, A.J., LAZDUNSKI, M. & HONORE, E. (1997). $K_V2.1/K_V9.3$, a novel ATP-dependent delayed rectifier K^+ channel in oxygen-sensitive pulmonary artery myocytes. *EMBO J.*, **16**, 6615–6625.

PEREZ-GARCIA, M.T., LOPEZ-LPPEZ, J.R., RIESCO, A.M., HOPPE, U.C., MARBAN, E., GONZALEZ, C. & JOHNS, D.C. (2000). Viral gene transfer of dominant-negative K_V4 construct suppresses an O_2-sensitive K^+ current in chemoreceptor cells. *J. Neurosci.*, **20**, 5689–5695.

PLATOSHYN, O., YU, Y., GOLOVINA, V.A., MCDANIEL, S.S., KRICK, S., LI, L., WANG, J.Y., RUBIN, L.J. & YUAN, J.X. (2001). Chronic hypoxia decreases K(V) channel expression and function in pulmonary artery myocytes. *Am. J. Physiol.*, **280**, L801–L812.

RETTIG, J., HEINEMANN, S.H., WUNDER, F., LORRA, C., PARCEI, D.N., DOLLY, J.O. & PONGS, O. (1994). Inactivation properties of voltage-gated K^+ channels altered by presence of β-subunit. *Nature*, **369**, 289–294.

RUDY, B., SEN, K., VEGA-SAENZ DE MIERA, E., LAU, D., RIED, T. & WARD, D.C. (1991). Cloning of a human cDNA expressing a high voltage-activating, TEA-sensitive, type-A K^+ channel which maps to chromosome 1 band p21. *J. Neurosci. Res.*, **29**, 401–412.

SCHROTER, K.H., RUPPERSBERG, J.P., WUNDER, F., RETTIG, J., STOCKER, M. & PONGS, O. (1991). Cloning and functional expression of a TEA-sensitive A-type potassium channel from rat brain. *FEBS Lett.*, **278**, 211–216.

SERODIO, P., KENTROS, C. & Rudy, B. (1994). Identification of molecular components of A-type channels activating at subthreshold potentials. *J. Neurosci.*, **72**, 1516–1529.

SMIRNOV, S.V., BECK, R., TAMMARO, P., ISHII, T. & AARONSON, P.I. (2002). Electorophysiologically distinct smooth muscle cell subtypes in rat conduit and resistance pulmonary arteries. *J. Physiol.*, **538**, 867–878.

STUHMER, W., RUPPERSBERG, J.P., SCHROTER, K.H., SAKMANN, B., STOCKER, M., GIESE, K.P., PERSCHKE, A., BAUMANN, A. & PONGS, O. (1998). Molecular basis of functional diversity of voltage-gated potassium channels in mammalian brain. *EMBO. J.*, **8**, 3235–3244.

TERASAWA, K., NAKAJIMA, T., IIDA, H., IWASAWA, K., OONUMA, H., JO, T., NAKAMURA, F., FUJIMORI, Y., TOYO-OKA, T. & NAGAI, R. (2002). Nonselective cation currents regulate membrane potential of rabbit coronary arterial cell: modulation by lysophoshatidylcholine. *Circulation*, **106**, 3111–3119.

TURNER, J.L. & KOZLOWSKI, R.Z. (1997). Relationship between membrane potential, delayed rectifier K^+ currents and hypoxia in rat pulmonary arterial myocytes. *Exp. Physiol.*, **82**, 629–645.

WANG, I., JUHASZOVA, M., CONTE, J.V., GAINE, S.P., RUBIN, L.J. & YUAN, J.X. (1998). Action of fenfluramine on voltage-gated K^+ channels in human pulmonary artery smooth muscle cells [letter]. *Lancet*, **352**, 290.

WEIR, E.K., REEVE, H.L., HUANG, J.M., MICHELAKIS, E., NELSON, D.P., HAMPAL, V. & ARCHER, S.L. (1996). Anorexic agents, aminorex, fenfluramine, and dexfenfluramine inhibit potassium current in rat pulmonary vascular smooth muscle and cause pulmonary vasoconstriction. *Circulation*, **94**, 2216–2220.

YAMASHITA, T., NAKAJIMA, T., HAMADA, E., HAZAMA, H., OMATA, M. & KURACHI, Y. (1995). Flecainide inhibits the transient outward current in atrial myocytes isolated from the rabbit heart. *J. Pharmacol. Exp. Ther.*, **274**, 315–321.

YEOLA, S.W. & SNYDERS, D.J. (1997). Electrophysiological and pharmacological correspondence between $K_V4.2$ current and rat cardiac transient outward current. *Cardiovasc. Res.*, **33**, 540–547.

YUAN, J.X. (2001). Oxygen-sensitive K^+ channels: where and what? *Am. J. Physiol.*, **281**, L1345–L1349.

YUAN, J.X., ALDINGER, A.M., JUHASZOVA, M., WANG, J., CONTE JR, J.V., GAINE, S.P., ORENS, J.B. & RUBIN, L.J. (1998). Dysfunctional voltage-gated K^+ channels in pulmonary artery smooth muscle cells of patients with primary pulmonary hypertension. *Circulation*, **98**, 1400–1406.

YUAN, X.J. (1995). Voltage-gated K^+ currents regulate resting membrane potential and $[Ca^{2+}]_i$ in pulmonary arterial myocytes. *Circ. Res.*, **77**, 370–378.

YUAN, X.J., GOLDMAN, W.F., TOD, M.L., RUBIN, L.J. & BLAUSTEIN, M.P. (1993). Ionic currents in rat pulmonary and mesenteric arterial myocytes in primary culture and subculture. *Am. J. Physiol.*, **264**, L107–L115.

YUAN, X.J., WANG, J., JUHASZOVA, M., GOLOVINA, V.A. & RUBIN, L.J. (1998). Molecular basis and function of voltage-gated K^+ channels in pulmonary arterial smooth muscle cells. *Am. J. Physiol.*, **274**, L621–L635.

(Received October 26, 2004
Revised March 17, 2005
Accepted April 22, 2005
Published online 6 June 2005)

ARTICLE IN PRESS

Available online at www.sciencedirect.com

SCIENCE DIRECT®

Life Sciences

ELSEVIER

Life Sciences xx (2005) xxx – xxx

www.elsevier.com/locate/lifescie

Endogenous prostaglandin D_2 synthesis decreases vascular cell adhesion molecule-1 expression in human umbilical vein endothelial cells

Hideyuki Negoro [a,*], Wee Soo Shin [a,b], Rie Hakamada-Taguchi [b], Naomi Eguchi [c], Yoshihiro Urade [c], Atsuo Goto [a], Teruhiko Toyo-oka [a,b], Toshiro Fujita [a], Masao Omata [a], Yoshio Uehara [a,b]

[a] *Department of Medicine #2, University of Tokyo, 7-3-1 Hongo, Bunkyo, Tokyo 113-0033, Japan*
[b] *Health Service Center, University of Tokyo, Tokyo 113-0033, Japan*
[c] *Osaka Bioscience Institute, Suita, Osaka, Japan*

Received 23 August 2004; accepted 24 February 2005

Abstract

We examined the role of prostaglandin D_2 (PGD_2) in the expression of vascular cell adhesion molecule-1 (VCAM)-1 following interleukin-1β (IL-1) stimulation in human umbilical vein endothelial cells (HUVEC) transfected with lipocaline-type PGD_2 synthase (L-PGDS) genes. HUVEC were isolated from human umbilical vein and incubated with 20 U/ml IL-1 and various concentrations of authentic PGD_2. The isolated HUVEC were also transfected with L-PGDS genes by electroporation. The L-PGDS-transfected HUVEC were used to investigate the role of endogenous PGD_2 in IL-1-stimulated VCAM-1 biosynthesis. We also used an anti-PGD_2 antibody to examine whether an intracrine mechanism was involved in VCAM-1 production. PGD_2 and VCAM-1 levels were determined by radio- and cell surface enzyme-immunoassay, respectively. VCAM-1 mRNA was assessed by RT-PCR. IL-1-stimulated VCAM-1 expression by HUVEC was dose-dependently inhibited by authentic PGD_2. L-PGDS gene-transfected HUVEC produced more PGD_2 than HUVEC transfected with the reporter gene alone. IL-1 induced increases in VCAM-1 expression in HUVEC transfected with reporter genes alone. However, this effect was significantly attenuated in the case of IL-1 stimulation of HUVEC transfected with L-PGDS genes, and accompanied by an apparent suppression of VCAM-1 mRNA expression. Neutralization of extracellular PGD_2 by anti-PGD_2-specific antibody influenced neither VCAM-1 mRNA expression nor VCAM-1 biosynthesis. In conclusion, HUVEC transfected with L-PGDS genes showed increased PGD_2 synthesis. This increase was associated with attenuation of both VCAM-1 expression and VCAM-1 mRNA expression. The results suggest that endogenous PGD_2 decreases VCAM-1 expression and VCAM-1 mRNA expression, probably through an intracrine mechanism.

Keywords: Prostaglandin D_2; Prostaglandin D_2 synthase; Vascular cell adhesion molecule-1; Gene transfer

Introduction

The hypothesis proposed by Ross and its modifications have been generally accepted as a mechanism of atherosclerosis where adhesion of circulating monocytes and lymphocytes to vascular endothelium presumably initiates a series of events toward atherosclerosis (Joris et al., 1983). Recent studies have disclosed further that to anchor leukocytes onto the endothelial cells, the adhesion molecules expressed on the surface of endothelial cells necessitated to bind to their ligands expressed on leukocytes. The adhesion molecules expressed on the endothelial cells include vascular cell adhesion molecule (VCAM)-1, intracellular adhesion molecule (ICAM)-1, P-selectin and E-selectin (Cybulsky and Gimbrone, 1991). Among them, VCAM-1 induced by interleukin (IL)-1 and tumor necrosis factor (TNF)-alpha play a key role in the adhesion of monocytes and lymphocytes on the endothelial cells (Faggio et al., 1990). In fact, VCAM-1 is demonstrated to occur in atherosclerotic lesions in the coronary artery of humans (O'Brien et al., 1990). Hence, VCAM-1 is believed to be a key factor for the development of immune-mediated cardiovascular injury.

* Corresponding author. Tel.: +81 3 3815 5411x3056; fax: +81 3 3814 0021.
E-mail address: negoro-2im@h.u-tokyo.ac.jp (H. Negoro).

0024-3205/$ - see front matter © 2005 Elsevier Inc. All rights reserved.
doi:10.1016/j.lfs.2005.02.037

Interestingly, we have recently reported that PGD_2 attenuates inducible nitric oxide generation in vascular smooth muscle cells (Nagoshi et al., 1998). Endogenous prostaglandin D_2 synthesis reduces plasminogen activator inhibitor-1 generation following cytokine stimulation in bovine endothelial cells (Negoro et al., 2002). Moreover, lipocalin-type PGD_2 synthase (L-PGDS) is demonstrated to occur in atheromatous lesions in the cardiovascular system (Eguchi et al., 1997) and PGD_2 is synthesized in vascular components of atheromatous lesions including endothelial cells, macrophages, platelets, and mast cells (Watanabe et al., 1982). These data strongly suggest that L-PGDS/PGD_2 is upregulated in response to immune-related vascular lesions and in turn, this increase is exerted to attenuate the progression of the arterial remodeling.

Considering these data, we proposed the hypothesis that PGD_2 regulates VCAM-1 expression in endothelial cells, thereby contributing to leukocyte adhesion, an integral component of the development of vascular injury. However, there had been few data investigating the crosstalk between endogenous L-PGDS/PGD_2 system and the adhesion molecule expression by cytokines. Hence, in the present study, in order to test our hypothesis that L-PGDS/PGD_2 protects the vascular wall against immune-related injury, we examined the relationship between endogenous PGD_2 and VCAM-1 expression by endothelial cells and attempted to reveal its intracellular mechanism mediated by PGD_2 using L-PGDS gene-transfected endothelial cells in culture. We also examined whether the increases in intracellular PGD_2 synthesis influenced VCAM-1 mRNA expression and VCAM-1 biosynthesis observed following interleukin-1β (IL-1) stimulation.

Materials and methods

Materials

Eicosanoids and related compounds were purchased from Funakoshi chemicals (Tokyo, Japan). Arachidonic acid was purchased from Sigma (St. Louis, MO, USA). Recombinant murine IL-1 was purchased from R&D Systems (Minneapolis, MN, USA). Radioactively labeled materials were purchased from Amersham (Tokyo, Japan). A 3-kb gene for rat brain PGDS [(5*Z*,13*E*)-(15*S*)-9*a*, 11*a*-epidoxy-15-hydroxyprosta-5,13-dienoate D-isomerase, EC 5.3.99.2] was isolated from a rat genomic DNA library by plaque hybridization with cDNA for the PGDS enzyme, as described in our previous studies (Urade et al., 1989). A 3-kb *Bam*HI fragment of rat PGDS, which belongs to the lipocalin family, was inserted into a pcD2 plasmid containing the SV40 promoter, along with a polyA signal at the *Xho*I site (Invitrogen, Carlsbad, CA, USA) (Chen and Okayama, 1987). The β-galactosidase gene with a cytomegalovirus (CMV) promoter at an *Xba*I site was inserted into the pBluescript 2 KS+ plasmid (Stratagene, La Jolla, CA, USA).

Cell culture

Human umbilical vein endothelial cells (HUVEC) were harvested enzymatically as described previously (Zimmerman et al., 1990). They were maintained in medium 199 (GIBCO BRL, Gaithersburg, MD), containing Hepes, heparin (1%), endothelial cell growth factor (50 μg/ml), L-glutamine (1%), antibiotics, and 5% fetal bovine serum (FBS). When the cells reached confluence, they were replanted onto low pyrogen fibronectin at 20,000 cells/cm^2. HUVEC which were isolated from a confluent monolayer of polygonal cells. The cells expressed von Willbrand factor as determined by their content of specific mRNA and immunoreactive protein. Cellular viability was assessed by Trypan blue exclusion.

Effect of exogenous PGD2 on VCAM-1 expression in endothelial cells

Cultures of HUVEC were treated with 20 U/ml IL-1, according to the previous study (Negoro et al., 2002), in the presence of various concentrations of PGD2 or carbaprostacyclin, a stable PGI2 analogue to be incubated for 18 h. Thereafter, the HUVEC were washed three times with FBS-free Dulbecco's phosphate-buffered saline (D-PBS; Gibco) and the cells were re-incubated in 1 ml of fresh D-PBS for 2 h. Subsequently, the cells and culture supernatants were used in various assays.

Transfection of L-PGDS genes into HUVEC

HUVEC were transfected with L-PGDS genes using the Shimadzu GTE-10 electroporation device (Gene Transfer Equipment-10, Shimadzu Co., Ltd., Kyoto, Japan). This equipment transiently increases the permeability of plasma membranes of HUVEC, thereby facilitating translocation of genes into the cytoplasm. Briefly, the cells were washed three times with FBS-free D-PBS and 10 μg of pcD2-rat PGDS in 0.5 ml of fresh D-PBS were added to each well (Ohtani et al., 1989). A transient electrical current was applied onto HUVEC growing in the culture dishes, using a 35-mm round electrode (Model FTC-33D3, Shimadzu Co., Ltd., Kyoto, Japan), after which the cells were incubated for 30 min.

Following transfection, 2 ml of DMEM containing 10% FBS was added to the HUVEC and the dishes were incubated for an additional 24 h. Endogenous PGD_2 production was stimulated by adding 10^{-6} mol/l arachidonic acid for 24 h. Fresh medium containing 10^{-6} mol/l arachidonic acid was then added and VCAM-1 mRNA expression and VCAM-1 expression were stimulated for 18 h by the addition of 20 U/ml IL-1. At the end of this incubation period, the HUVEC were washed three times with FBS-free D-PBS and incubated in 1 ml of fresh D-PBS for 2 h. Finally, the cells and culture supernatants were collected for analysis. In addition, to confirm that the VCAM-1 expression following arachidonate stimulation was indeed mediated by PGs generation, we inhibited the endogenous PGs generation using 10^{-6} mol/l indomethacin and assessed the alterations of VCAM-1 formation.

For comparison, HUVEC were transfected with β-galactosidase genes (β-gal) by electroporation to determine the efficacy of gene transfection. Three days after the transfection, HUVEC were stained with X-gal (Bonnerot et al., 1987), and

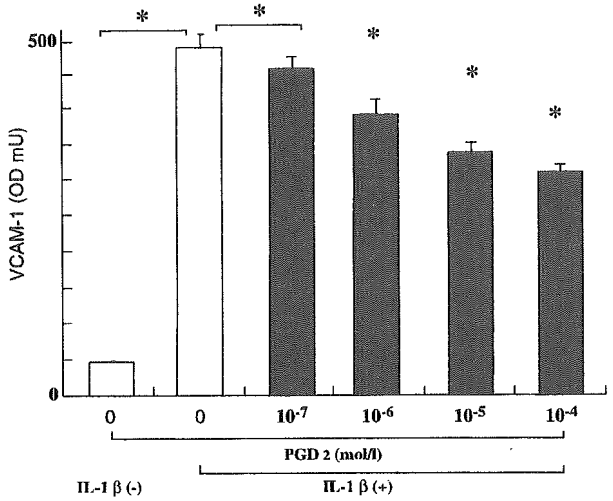

Fig. 1. Effect of exogenous PGD_2 on VCAM-1 expression in endothelial cells. Stimulation of endothelial cells with IL-1 significantly increased VCAM-1 expression (left two columns). The increase was reduced in a dose-dependent manner by the addition of PGD_2 at concentrations ranging from 10^{-7} to 10^{-4} mol/l. All experiments were performed three different times with at least six replicates. Statistical differences were analyzed by one-way ANOVA and Duncan's multiple range tests. $^*P<0.01$ vs. the value at 0 mol/L PGD_2. N.S. represents not statistically significant.

β-galactasidase expression was measured. Transfection efficacy was estimated as the ratio of the X-gal stained area to the sectional area of the HUVEC.

Neutralizing extrinsic PGD2 released from HUVEC

We attempted to neutralize PGD_2 using an anti-PGD_2-specific antibody in order to investigate the effects of PGD_2 released from L-PGDS-transfected HUVEC. We estimated the amount of anti-PGD_2 antibody required to completely neutralize the secreted PGD_2 using the Scatchard analysis. The binding affinity was 0.0051 ml/pg, and the B_{max} (maximal binding capacity) was 25 pg/l (Tobian et al., 1985). Therefore, 1 l of antibody had the capacity to bind 25 pg PGD_2. Taking into account of these results, we used 200 μl of the antibody to inhibit the receptor-mediated actions of PGD_2 in HUVEC under our culture conditions. The anti-PGD_2 antibody was raised in our laboratories using PGD_2-conjugated thyroglobulin and Freund's complete adjuvant. The antibody cross-reacted 0.003% with thromboxane B_2, 0.01% with prostaglandin E_2 (PGE_2), 0.009% with prostaglandin $F_{2\alpha}$ ($PGF_{2\alpha}$), 0.008% with 6-keto-$PGF_{1\alpha}$ and 0.01% with arachidonate (Uehara et al., 1987). Antibody activity was confirmed by suppression of intracellular cyclic AMP (cAMP) following PGD_2 stimulation via PGD_2 receptor, which acts as a second messenger for PGD_2 signal transduction (Koide et al., 1993).

Eicosanoid radioimmunoassay

Eicosanoids were determined in culture media using the direct radioimmunoassay method described previously (Uehara et al., 1987). Briefly, 0.1 ml of sample, 0.1 ml of [^{3}H] eicosanoid (5000 dpm) and 0.1 ml of the diluted antibody were mixed and incubated at 4 °C for 24 h. To separate bound from free [^{3}H] eicosanoid, 0.1 ml of dextran-coated charcoal in a 50-mmol/l phosphate buffer at pH 7.4 containing 0.1% gelatin and 100 mmol/l NaCl was added to the ice-chilled assay mixture. The mixture was vortexed and centrifuged at 3000 rpm for 5

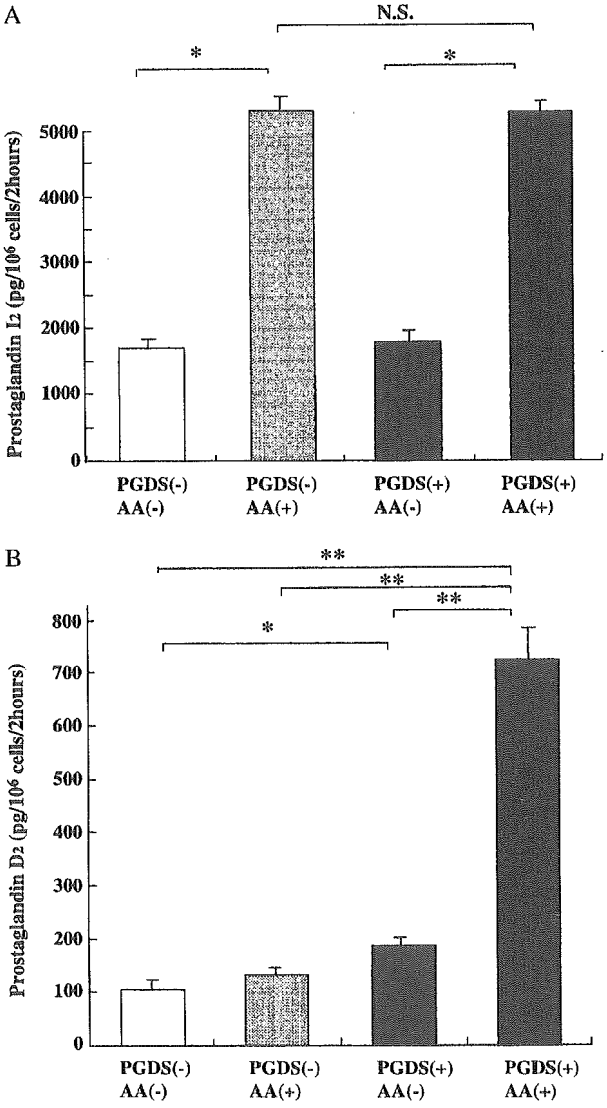

Fig. 2. PGI_2 and PGD_2 generation in endothelial cells. PGI_2 was assayed as 6-keto-$PGF_{1\alpha}$ using radioimmunoassay. In arachidonate (AA)-free media, there were no differences in PGI_2 generation between endothelial cells having only reporter genes (PGDS(−), AA(−)), and those having L-PGDS genes (PGDS(+), AA(−)) (Graph A). The addition of 10^{-6} mol/L arachidonate to the cultures increased PGI_2 generation; however, there were no differences in PGI_2 production between PGDS(−), AA(+) and PGDS(+), AA(+) lines. In contrast to the results with PGI_2, 10^{-6} mol/l arachidonate did not stimulate PGD_2 generation in cells having reporter genes alone (two columns to the left in Graph b). However, cells carrying the L-PGDS genes acquired the ability to produce PGD_2 in response to arachidonate stimulation (two columns to the right in Graph B). Statistical differences were assessed by Student's t-test ($n=6$). $^*P<0.01$, $^{**}P<0.001$. N.S. represents not statistically significant.

min at 4 °C. The supernatant was assayed for [^{3}H]eicosanoids bound to the antibody. Radioactivity was determined using an automatic liquid scintillation counter. The properties of the anti-6keto-$PGF_{1\alpha}$ antibody was described previously (Tobian et al., 1985; Uehara et al., 1987). The cross-reactivity and its properties of the anti-PGD_2 antibody was detailed above. The low cross-reactivity of each antibody made it feasible to measure directly the eicosanoid in media.

VCAM-1 and VCAM-1 mRNA measurements

We measured VCAM-1 expression by cell surface enzyme immunoassay as described previously (Caterina et al., 1995). Briefly, we incubated HUVEC first with saturating concentrations of specific monoclonal antibodies against the VCAM-1, then with biotinylated goat anti-mouse IgG (Vector Labs, Inc., Burlingame, CA, USA), and finally with streptavidin-alkaline phosphatase (ZymedLaboratories, Inc., South San Francisco, CA, USA). Cells were washed three times between each incubation step. The surface expression of each protein was quantified spectrophotometrically reading the optical density of the wells (410 nm) 15–60 min after the addition of chromogenic substrate.

Cultured VCAM-1 transcripts were detected using the reverse transcription-polymerase chain reaction (RT-PCR) method as described previously (Tamasawa et al., 2001). Briefly, we extracted total RNA from endothelial cells by the standard acid guanidinium isothiocyanate method, and used the reverse-transcribed cDNA as a template for PCR. The primer sequences for VCAM-1 were: upper strand, 5′-AATTTATGTGTGTGAAGGAG-3′; and lower strand, 5′-GCATGTCATATTCACAGAA-3′. The expressed size of PCR products was 740 bp for VCAM-1. The annealing/elongation/denaturation conditions for the PCR reaction were 55 °C/72 °C/94 °C, respectively, for a total of 30 cycles of 30 s each, with an initial 5 min denaturation step at 94 °C and an ultimate 10 min extension step at 72 °C. The reaction products were separated by agarose gel electrophoresis and stained with ethidium bromide.

Statistical analysis

All values are expressed as the mean ± S.E. The differences between values were assessed by an one-way ANOVA and Duncan's multiple range test using the STATISTICA program (StatSoft, Tulsa, OK, USA) on a Gateway G6-400 computer system (Gateway Inc., N Sioux City, SD, USA) running the Windows 98 operating system. P values less than 0.05 were considered statistically significant.

Results

Effect of exogenous PGD2 on VCAM-1 expression in endothelial cells

Stimulation of endothelial cells with IL-1 significantly increased VCAM-1 expression (Fig. 1). The increase was reduced in a dose-dependent manner by the addition of PGD_2 at concentrations ranging from 10^{-7} to 10^{-4} mol/l.

In contrast to PGD_2, the VCAM-1 expression by HUVEC following IL-1 stimulation was not affected at all by 10^{-5} mol/l carbaprostacyclin (488.2±17.4 versus 486.3±19.5 OD mU, not significant, N.S.). In addition, exogenous PGD_2 also reduced monocyte chemoattractant protein-1 expression by HUVEC following stimulation in a dose-dependent manner (data not shown).

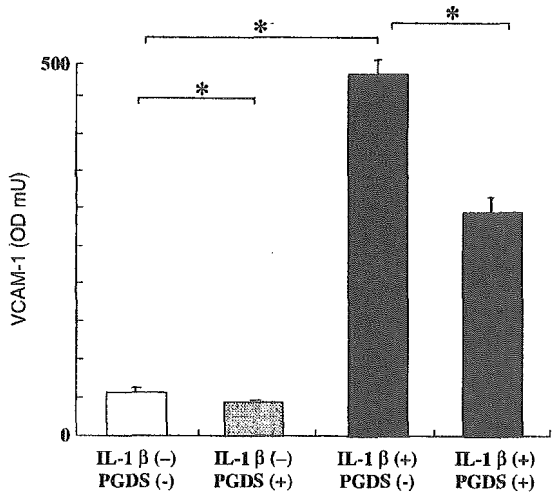

Fig. 3. Effect of PGD_2 synthase gene transfection on VCAM-1 expression in endothelial cells. Under normal (unstimulated) conditions, endothelial ells bearing L-PGDS genes (IL-1(−), PGDS(+)) expressed less VCAM-1 than those bearing reporter genes alone (IL-1(−), PGDS(−)). VCAM-1 expression increases observed following IL-1 stimulation were significantly attenuated in cells carrying L-PGDS genes in response to arachidonic acid stimulation (IL-1(+), PGDS(+), AA(+)), though there was no attenuation of VCAM-1 expression in cells carrying L-PGDS genes but not stimulated by arachidonic acid (IL-1(+), PGDS(+), AA(−)), compared to endothelial cells having only reporter genes (IL-1(+), PGDS(−)). The experiment was carried out in the presence of 10^{-6} mol/l arachidonate. Statistical differences were assessed by Student's t-test ($n=6$). *$P<0.01$.

Gene transfection and eicosanoid generation in HUVEC

We transfected HUVEC with L-PGDS genes in order to increase endogenous PGD_2 formation. The transfection efficiency of the genes was 39.8±0.45. Basal levels of prostacyclin (PGI_2), the major eicosanoid synthesized in HUVEC, were 1738±95 pg/10^6 cells/2 h in cells having reporter genes alone under arachidonate-free conditions. The PGI_2 generation was a markedly increased by 240% when the cells were stimulated with 10^{-6} mol/l arachidonate (Fig. 2A). L-PGDS gene transfection did not influence PGI_2 synthesis in HUVEC maintained under either arachidonate-free or arachidonate-stimulated conditions, as compared to HUVEC transfected with reporter genes.

The basal levels of PGD_2 in reporter-gene-transfected HUVEC maintained in arachidonate-free media were as low as 102.3±16.1 pg/10^6 cells/2 h, and the addition of 10^{-6} mol/l arachidonate had no effect on PGD_2 synthesis. In contrast, L-PGDS gene-transfected HUVEC showed an increase (70.2%) in PGD_2 generation even in arachidonate-free media, as compared with control HUVEC carrying reporter genes alone. Furthermore, 10^{-6} mol/l arachidonate markedly stimulated PGD_2 biosynthesis by 602.0%, as compared with control HUVEC carrying vector genes alone (Fig. 2B). These data clearly suggest that the L-PGDS genes alter the phenotype of HUVEC so that the recombinant cells acquire the capacity to produce PGD_2 in response to arachidonate stimulation. It is noteworthy that the PGD_2 production levels achieved in arachidonate-stimulated HUVEC carrying L-PGDS genes were far below the concentrations in media, that are required to decrease IL-1-stimulated VCAM-1 expression (Fig. 1).

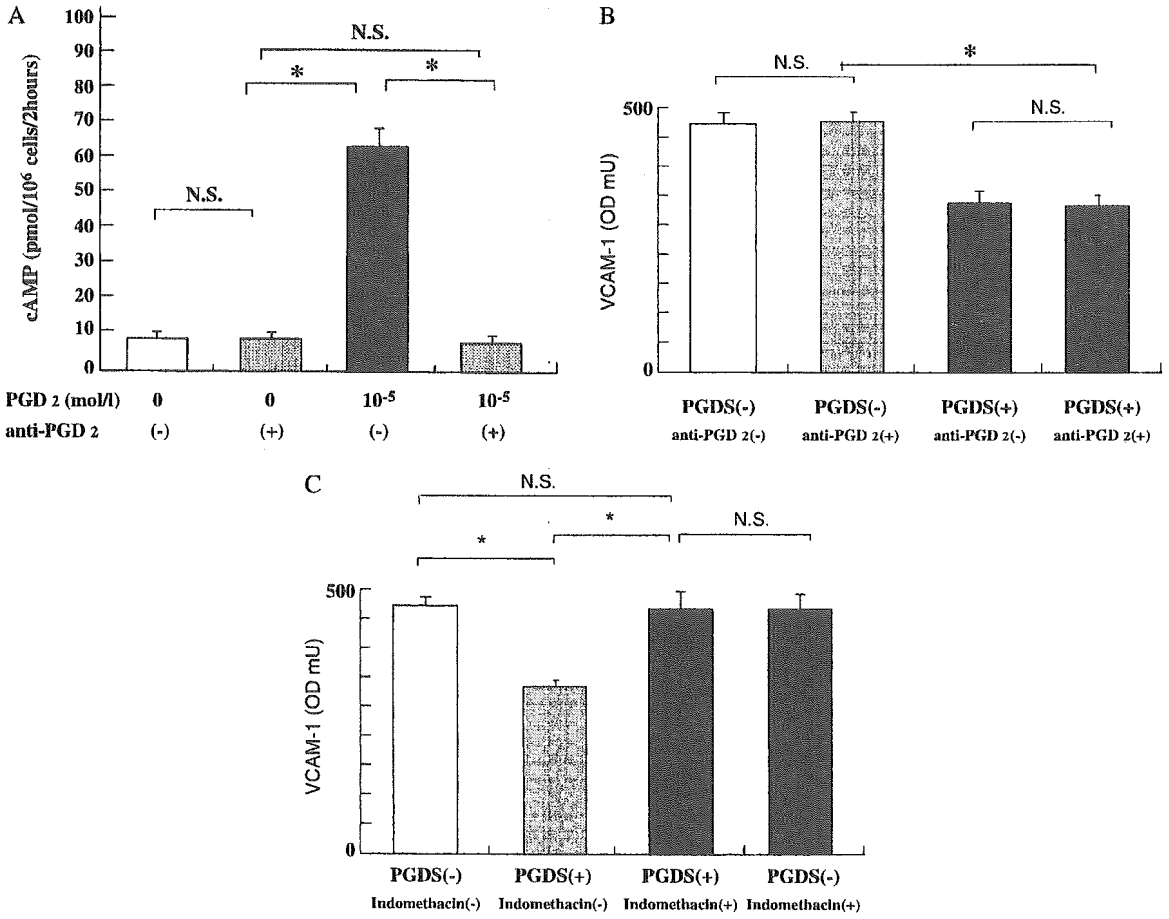

Fig. 4. Effect of PGD_2 on VCAM-1 expression in endothelial cells. cAMP levels were measured to assess the antibody inhibition of PGD_2 receptor-mediated signal transduction in the cells with transporter gene alone (Graph A). 10^{-5} mol/l PGD_2 greatly increased cAMP formation in the cells in the absence of anti-PGD_2 antibody (anti-PGD_2(−)). This increase was completely abolished to the basal levels by the addition of anti-PGD_2 antibody in the media. Using such a dose of anti-PGD_2 antibody, we examined the effects of neutralization of PGD_2 in media on VCAM-1 expression (Graph B). VCAM-1 expression following IL-1 stimulation was significantly reduced in endothelial cells having L-PGDS genes and without anti-PGD_2 antibody (PGDS(+), anti-PGD_2(−)), compared to endothelial cells with reporter genes alone (PGDS(−), anti-PGD_2(−)). The reduction in VCAM-1 expression was unaffected when PGD_2 in the culture was neutralized with an anti-PGD_2-specific antibody (PGDS(+), anti-PGD_2(+)). 10^{-6} mol/l indomethacin, a potent cyclooxygenase inhibitor, reversed toward the basal levels the reduction of VCAM-1 expression following IL-1 stimulation of HUVEC transfected with L-PGDS gene (Graph C). These studies were carried out in the presence of 10^{-6} mol/l arachidonate. Statistical differences were assessed by Student's *t*-test. $^*P<0.01$. N.S. represents not statistically significant.

Effect of L-PGDS gene transfection on VCAM-1 expression in HUVEC

Using the HUVEC having L-PGDS genes, we investigated the effects of endogenous PGD_2 on the expression of VCAM-1 with or without IL-1 stimulation. The VCAM-1 expression was significantly increased upon IL-1 stimulation in endothelial cells transfected with transporter genes. This increase in VCAM-1 with or without IL-1 stimulation was significantly blunted in HUVEC transfected with L-PGDS genes that produced indeed endogenous PGD_2 in response to arachidonate stimulation (Fig. 3).

Intracellular effects of PGD_2 on VCAM-1 expression

In order to assess the role of PGD_2 receptor-mediated signal transduction in VCAM-1 expression, we studied changes in cAMP, a second messenger of PGD_2 signal transduction in HUVEC transfected with transporter gene alone. Intracellular cAMP was unaffected by L-PGDS transfection per se. However, intracellular cAMP was increased by exogenous PGD_2 stimulation. This response was completely abrogated by addition of anti-PGD_2 antibody to the media, the amount of which was more than the concentrations sufficient to neutralize PGD_2 in the media (Fig. 4A). Moreover, it is noted that the PGD_2 levels produced by the HUVEC carrying L-PGDS genes were much lower than the concentrations of exogenous PGD_2 required to decrease the VCAM-1 expression.

Using such a dose of anti-PGD_2 antibody enough to inhibit the receptor-mediated cyclic AMP rising, we investigated contribution of PGD_2 receptor-mediated signal transduction to the PGD_2-mediated VCAM-1 expression, and determined VCAM-1 expression in the supernatants following neutralization with an anti-PGD_2-specific antibody. The addition of anti-PGD_2 antibody to the media did not influence VCAM-1 expression following IL-1 stimulation in the endothelial cells transfected with L-PGDS genes (Fig. 4B).

Moreover, 10^{-6} mol/l indomethacin, a potent cyclooxygenase inhibitor, reversed toward the basal levels the reduction of VCAM-1 expression following IL-1 stimulation of HUVEC transfected with L-PGDS gene (Fig. 4C). These results clearly indicated that anti-PGD_2-specific antibody inhibited the PGD_2 receptor-mediated signal transduction and that PGD_2-mediated reduction in VCAM-1 expression was not due to the PGD_2 receptor-mediated events.

L-PGDS genes and expression of VCAM-1 mRNA

We demonstrated that L-PGDS gene transfection onto HUVEC brought about increases in PGD_2 formation and decreases in VCAM-1 expression. Hence, we examined whether the negative effect on VCAM-1 expression was associated with reduced levels of VCAM-1 mRNA (Fig. 5). The expression of VCAM-1 mRNA following IL-1 stimulation was significantly less in the HUVEC carrying L-PGDS genes (upper graph). The reduction of VCAM-1 mRNA signals by L-PGDS genes was observed even when PGD_2 was neutralized by the anti-PGD_2 specific antibody (lower graph).

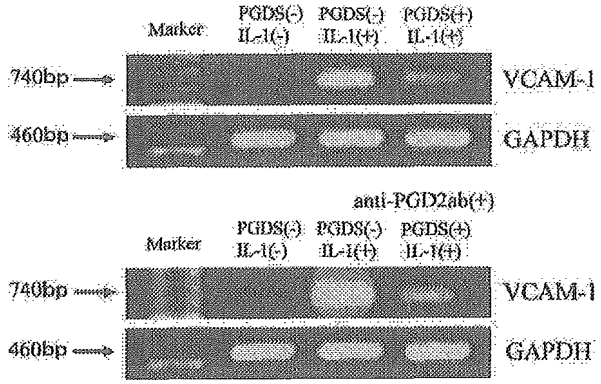

Fig. 5. Effect of PGD_2 synthase gene transfection on VCAM-1 mRNA. Changes in VCAM-1 mRNA levels were investigated using RT-PCR. VCAM1-1 mRNA signals following IL-1 stimulation in the cells having transporter gene alone (PGDS(−)) (middle lane in upper graph) was attenuated in the cells having L-PGDS gene (PGDS(+)) (right lane in upper graph). This reduction in the signals was also observed even if PGD_2 in media was neutralized by anti-PGD_2 antibody, the dose of which was enough to decrease cAMP increase by 10^{-5} mol/l PGD_2 (PGDS(+), antiPGD_2ab(+)) (right lane in lower graph). The experiment was repeated three times. The results corresponded to the data presented in this figure.

Discussion

In the present study, we demonstrated that PGD_2 regulates VCAM-1 expression in HUVEC following IL-1 stimulation. Importantly, we also demonstrated that endogenous PGD_2 production in HUVEC transfected with L-PGDS genes brought about a decrease of VCAM-1 expression. This effect was observed even if the PGD_2-mediated cAMP increase was reversed to basal levels using anti-PGD_2-specific antibody. These findings strongly suggest that PGD_2 exerts inhibitory effects on VCAM-1 expression via an intracellular mechanism as well as the well-known receptor-mediated mechanism (Zidovetzki et al., 1999).

In this context, recent studies have demonstrated that the orphan nuclear receptor of peroxysome proliferator-activated receptor (PPAR)-γ, a member of the nuclear receptor superfamily of ligand-dependent transcription factors, binds to PGD_2 metabolites and thereby regulates adipocyte differentiation and glucose homeostasis (Forman et al., 1995; Kliewer et al., 1995).

PGD_2 is converted quickly to PGJ_2, delta 12-PGJ_2, and 15-deoxy-delta12,14 PGJ_2 in plasma (Kikwa et al., 1984). 15-Deoxy-delta12,14 PGJ_2 inhibits inhibitor of κB kinase that phosphorylates another inhibitor of κB after activation with cytokines and also affects the DNA-binding domains of NF-κB subunits (Ricote et al., 1998). Because the genes involved in VCAM-1 expression include the nuclear factor-κB (NF-κB) binding site in its promoter regions (Collins et al., 1995), it is presumable that PGD_2 and its metabolites inhibit cytokine-induced VCAM-1 expression, at least in part, through inhibition of NF-κB translocation.

It is reported that VCAM-1 mRNA and VCAM-1 are much expressed in vascular lesions such as atherosclerosis (O'Brien

et al., 1990). Different cell lines like macrophages, platelets or lymphocytes work together to secrete cytokines in response to the inflammatory events, and in turn, the secreted cytokines stimulate the endothelial cells, thereby increasing VCAM-1 mRNA and VCAM-1 expression in the atherosclerotic lesions. In fact, it is well postulated that L-PGDS is highly expressed in the stenotic lesions and in the lipid core of advanced atherosclerotic plaques in patients with stable angina (Eguchi et al., 1997). Moreover, PGD_2 reduces inducible nitric oxide synthase formation. These actions of PGD_2 and metabolites on vasoactive substances regulated by cytokines are in favor of vascular protection against vascular injury (Nagoshi et al., 1998).

The endothelial cells exhibited a striking increase in PGI_2 generation, but not PGD_2, following arachidonate stimulation, suggesting that these cells have a large capacity to synthesize PGI_2, but not PGD_2. In spite of this, L-PGDS gene transfection greatly enhanced PGD_2 synthesis in EC. This was particularly apparent when eicosanoid expression was stimulated with its precursor, arachidonate. The alteration of phenotype of these cells reduced VCAM-1 mRNA expression and consequently VCAM-1 expression. This genetic procedure would provide a new strategy against vascular lesions.

The VCAM-1 expression in L-PGDS gene-transfected endothelial cells, which are capable of synthesizing endogenous PGD_2, was 39% less than that of control endothelial cells with only reporter genes. Considering the efficacy of gene transfection, as estimated from reporter gene transfection, this reduction in VCAM-1 expression corresponds to the complete elimination of VCAM-1 expression in L-PGDS gene-transfected endothelial cells. These data suggest that marginal transfection is enough to reduce VCAM-1 expression, or that the transfected cells influence the activities of neighboring cells. These activities have relevance to the in vivo situation, and remain to be clarified.

In conclusion, the introduction of PGD_2 synthase genes into endothelial cells increased endogenous PGD_2 generation. This brought about a reduction in VCAM-1 expression and a decrease in VCAM-1 mRNA expression following IL-1 stimulation. The inhibitory effects of PGD_2 on VCAM-1 expression were due to an intracrine mechanism rather than to any receptor-mediated events. Since suppression of the VCAM-1 system is postulated to be protective, an increase in endogenous PGD_2 synthesis might represent a novel strategy to prevent cardiovascular injury in humans.

Acknowledgements

The authors acknowledge Yukari Kawabata and Chieko Henmi for technical assistance.

References

Bonneroi, C., Rocancourt, D., Briani, P., Grimber, G., Nicolas, J.F., 1987. A b-galactosidase hybrid protein targeted to nuclei as a marker for developmental studies. Proceedings of the National Academy of Sciences of the United States of America 84, 6795–6799.

Caterina, R.D., Libby, P., Peng, H., Thannickal, V.J., Rajavashisth, T.B., Gimbrone, M.A., Shin, W.S., Liao, J.K., 1995. Nitric oxide decreases cytokine-induced endothelial activation. Journal of Clinical Investigation 96, 60–68.

Chen, C., Okayama, H., 1987. High-efficiency transformation of mammalian cells by plasmid DNA. Molecular and Cellular Biology 7, 2745–2752.

Collins, T., Read, M.A., Neish, A.S., Whitley, M.Z., Thanos, D., Maniatis, T., 1995. Transcriptional regulation of endothelial cell adhesion molecules: NF-kB and cytokine-inducible enhancers. FASEB Journal 9, 899–909.

Cybulsky, M.I., Gimbrone Jr., M.A., 1991. Endothelial expression of a mononuclear leukocyte adhesion molecule, in rabbit aortic endothelium. Science 251, 788–791.

Eguchi, Y., Eguchi, N., Oda, H., Seiki, K., Kijima, Y., Matsu-ura, Y., 1997. Expression of lipocalin-type prostaglandin D synthase (beta-trace) in human heart and its accumulation in the coronary circulation of angina patients. Proceedings of the National Academy of Sciences of the United States of America 94, 14689–14694.

Faggio, A., Ross, R., Harker, L., 1990. Studies of hypercholesterolemia in the nonhuman primate: I. Changes that lead to fatty streak formation. Arteriosclerosis 4, 323–340.

Forman, B.M., Tontonoz, P., Chen, J., Brun, R.P., Spiegelman, B.M., Evans, R.M., 1995. 15-Deoxy-D12,14-prostaglandin J2 is a ligand for the adipocyte determination factor PPAR. Cell 83, 803–812.

Joris, I., Zand, T., Nunnari, J.J., Krolikowski, F.J., Majno, G., 1983. Studies on the pathogenesis of atherosclerosis: I. Adhesion and emigration of mononuclear cells in the aorta of hypercholesterolemic rats. American Journal of Pathology 113, 341–358.

Kikwa, Y., Narumiya, S., Fukushima, M., Wakatsuka, H., Hayaishi, O., 1984. 9-Deoxy-d9,d12-13,14-dihydroprostaglandin D_2, a metabolite of prostaglandin D_2 formed in human plasma. Proceedings of the National Academy of Sciences of the United States of America 81, 1317–1321.

Kliewer, S.A., Lenhard, J.M., Willson, T.M., Patel, I., Morris, D.C., Lehmann, J.M., 1995. A prostaglandin J2 metabolite binds peroxysome proliferator–activator g and promotes adipocyte differentiation. Cell 83, 813–819.

Koide, M., Kawahara, Y., Nakayama, I., Tsuda, T., Yokoyama, M., 1993. Cyclic AMP-elevation agents induce an inducible type of nitric oxide synthase in cultured vascular smooth muscle cells. Journal of Biological Chemistry 268, 24959–24966.

Nagoshi, H., Uehara, Y., Kanai, F., Maeda, S., Ogura, T., Goto, A., Omata, M., 1998. Prostaglandin D_2 inhibits inducible nitric oxide synthase expression in rat smooth muscle cells. Circulation Research 82, 204–209.

Negoro, H., Shin, W.S., Taguchi, R.H., Eguchi, N., Urade, Y.Goto, Toyo-oka, T., Fujita, T., Omata, M., Uehara, Y., 2002. Endogenous prostaglandin D_2 synthesis reduces an increase in plasminogen activator inhibitor-1 following interleukin stimulation in bovine endothelial cells. Journal of Hypertension 20, 1347–1354.

O'Brien, K.D., Allen, M.D., McDonald, T.O., Chait, A., Harlan, J.M., Fishbein, D., McCarthy, J., Ferguson, M., Hudkins, K., Bebjamin, C.D., Lobb, R., Alpers, C.E., 1990. Vascular cell adhesion molecule-1 is expressed in human coronary atherosclerotic plaques: implications for the mode of progression. Molecular and Cellular Endocrinology 68, 1–19.

Ohtani, K., Nakamura, M., Saito, S., Nagata, K., Sugamura, K., Hinuma, Y., 1989. Electroporation: application to human lymphoid cell lines for stable introduction of a transactivator gene of human T-cell leukemia virus type 1. Nucleic Acid Research 17, 1589–1604.

Ricote, M., Li, A.C., Willson, T.M., Kelly, C.J., Glass, C.K., 1998. The peroxysome proliferator-activated receptor-g is a negative regulator of macrophage activation. Nature 391, 79–82.

Tamasawa, N., Murakami, H., Matsui, J., Yamato, K., JingZhi, G., Imaizumi, T., Fujimoto, K., Yoshida, H., Satoh, K., Suda, T., 2001. An oxidised derivative of cholesterol increase the release of soluble vascular cell adhesion molecule-1 from human umbilical vein endothelial cells in culture. Biochimica et Biophysica Acta. General Subjects 1531, 178–187.

Tobian, L., Uehara, Y., Iwai, J., 1985. Prostaglandin alterations in barely hypertensive Dahl S rats. Transactions of the Association of the American Physiology 98, 378–383.

Uehara, Y., Tobian, L., Iwai, J., Ishii, M., Sugimoto, T., 1987. Alterations of vascular prostacyclin and thromboxane A2 in Dahl genetical strain susceptible to salt-induced hypertension. Prostaglandins 33, 727–738.

Urade, Y., Nagata, A., Suzuki, Y., Fujii, Y., Hayaishi, O., 1989. Primary structure of rat brain prostaglandin D synthase deducted from cDNA sequence. Journal of Biological Chemistry 264, 1041–1045.

Watanabe, T., Narumiya, S., Shimizu, T., Hayaishi, O., 1982. Characterization of the biosynthetic pathway of prostaglandin D_2 in human platelet-rich plasma. Journal of Biological Chemistry 257, 14847–14853.

Zidovetzki, R., Wang, J.L., Kim, J.A., Chen, P., Fisher, M., Hofman, F.M., 1999. Endothelin-1 enhances plasminogen activator-1 production by human brain endothelial cells via protein kinase C-dependent pathway. Arteriosclerosis, Thrombosis and Vascular Biology 19, 1768–1775.

Zimmerman, G.A., Whatley, R.E., McIntyre, T.M., Benson, D.E., Prescott, S.M., 1990. Endothelial cells for studies of platelet-activating factor and arachidonate metabolites. Methods in Enzymology 187, 520–535.

Gene Therapy (2005) 12, 203–210

www.nature.com/gt

RESEARCH ARTICLE

Efficient and stable Sendai virus-mediated gene transfer into primate embryonic stem cells with pluripotency preserved

K Sasaki[1,2], M Inoue[3], H Shibata[1], Y Ueda[3], S-i Muramatsu[4], T Okada[1], M Hasegawa[3], K Ozawa[1] and Y Hanazono[1]

[1]*Center for Molecular Medicine, Jichi Medical School, Minamikawachi, Tochigi, Japan;* [2]*Department of Plastic and Reconstructive Surgery, Faculty of Medicine, University of Tokyo, Bunkyo-ku, Tokyo, Japan;* [3]*DNAVEC Corporation, Tsukuba, Ibaraki, Japan; and* [4]*Department of Neurology, Jichi Medical School, Minamikawachi, Tochigi, Japan*

Efficient gene transfer and regulated transgene expression in primate embryonic stem (ES) cells are highly desirable for future applications of the cells. In the present study, we have examined using the nonintegrating Sendai virus (SeV) vector to introduce the green fluorescent protein (GFP) gene into non-human primate cynomolgus ES cells. The GFP gene was vigorously and stably expressed in the cynomolgus ES cells for a year. The cells were able to form fluorescent teratomas when transplanted into immunodeficient mice. They were also able to differentiate into fluorescent embryoid bodies, neurons, and mature blood cells. In addition, the GFP expression levels were reduced dose-dependently by the addition of an anti-RNA virus drug, ribavirin, to the culture. Thus, SeV vector will be a useful tool for efficient gene transfer into primate ES cells and the method of using antiviral drugs should allow further investigation for regulated SeV-mediated gene expression.
Gene Therapy (2005) **12**, 203–210. doi:10.1038/sj.gt.3302409
Published online 14 October 2004

Keywords: *primate embryonic stem cell; Sendai virus vector; gene transfer; green fluorescent protein; pluripotency; ribavirin*

Introduction

Since human embryonic stem (ES) cell lines have the ability to both proliferate indefinitely and differentiate into multiple tissue cells,[1,2] they are expected to have clinical applications as well as to serve as models for basic research and drug development. Although efficient and stable gene transfer into primate ES cells would be useful for such purposes, it has been difficult and only lentiviral vectors have been successful in achieving it.[3–5] We have previously developed Sendai virus (SeV) vectors that replicate in the form of negative-sense single-stranded RNA in the cytoplasm of infected cells and do not go through a DNA phase.[6] SeV vectors can efficiently introduce foreign genes without toxicity into airway epithelial cells,[7] vascular tissue,[8] skeletal muscle,[9] synovial cells,[10] retinal tissue,[11] and hematopoietic progenitor cells.[12] Here we report that the SeV-mediated gene transfer into primate ES cells is very efficient and stable even after the terminal differentiation of the cells. In addition, we show that SeV-mediated transgene expression levels can be reduced by the addition of a ribonucleoside analog, ribavirin, to the culture. Ribavirin is a mutagen and inhibitor of viral RNA polymerase.[13,14] It shows antiviral activity against a variety of RNA viruses and is used to treat infections of hepatitis C virus in combination with interferon-α[15,16] and of lassa fever virus.[17] The method of using antiviral drugs might offer a novel approach for regulated SeV-mediated gene expression in primate ES cells.

Correspondence: Dr Y Hanazono, Center for Molecular Medicine, Jichi Medical School, 3311-1 Yakushiji, Minamikawachi, Tochigi 329-0498, Japan
Received 20 April 2004; accepted 27 August 2004; published online 14 October 2004

Results

SeV-mediated gene transfer into ES cells

In this study, we have used an SeV vector, which is capable of self-replication but incapable of transmitting to other cells.[6] The vector does not encode the fusion (F) protein (Figure 1a), which is essential for viral entry into cells. It can be propagated only in a packaging cell line expressing the F protein. The green fluorescent protein (GFP) gene was introduced after the leader sequence of the vector genome. Cynomolgus ES cells[18] were exposed to the SeV vector for 24 h. Flow cytometric analysis at 2 days after infection showed that 15, 38, and 61% of cells fluoresced at 2, 10, and 50 transducing units (TU) per cell, respectively (Figure 1b). The gene transfer efficiency of about 60% is comparable to or even better than that for lentiviral vectors.[3] We confirmed that the undifferentiated cell fractions remained unchanged after the infection with SeV vector, as assessed by the expression of undifferentiated markers, alkaline phosphatase and SSEA-4 (data not shown). The GFP expression after infection was stable at least for a month. On the other hand, the GFP gene transfer to cynomolgus ES cells with adenovirus- and adeno-associated virus (AAV)-based vectors resulted in much lower expression levels (<20% by flow cytometry) and the levels declined to zero within a week after infection (Figure 1c).

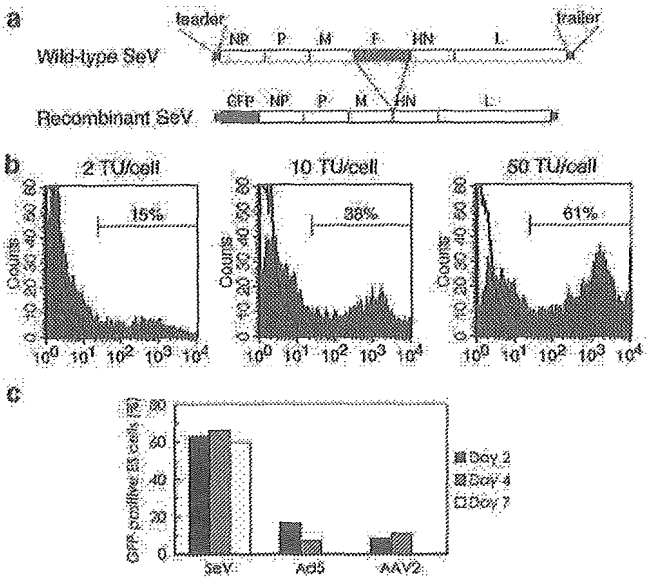

Figure 1 High-level transgene expression in cynomolgus ES cells after infection with SeV vector. (a) Schematic diagrams of the wild-type SeV genome and recombinant F-defective SeV carrying the GFP gene (SeV vector in this study). The SeV genome is 15 384 nucleotides long and its genes (NP, P, M, F, HN, and L) are in order from 3′ to 5′ in the negative-strand RNA. In the SeV vector, the entire fusion (F) gene was removed and the GFP gene was introduced at a unique NotI site between the leader sequence and NP gene. (b) The GFP expression by the SeV vector in cynomolgus ES cells. Cynomolgus ES cells were infected with the SeV vector at 2, 10, and 50 TU/cell. The flow cytometric profiles at day-2 postinfection are shown in gray. The white areas indicate uninfected ES cells. The fractions of GFP-positive cells are indicated. (c) The GFP expression levels in cynomolgus ES cells infected with the SeV (50 TU/cell), adenovirus serotype 5 (Ad5, 3.4×10^2 g.c./cell), and AAV serotype 2 (AAV2, 2.4×10^4 g.c./cell) vectors. The fractions of GFP-positive cells were examined by flow cytometry at 2, 4, and 7 days postinfection.

We plucked fluorescent ES cell colonies under a fluorescent microscope once at 1 month after infection and propagated them. After this selection procedure, approximately 90% of the ES cells expressed GFP (Figure 2a and b) and the high-level expression was stable for a year as assessed by flow cytometry (Figure 2c, upper). The mean fluorescence intensity per cell was also stable (Figure 2c, lower), indicating that the replicating vector genome was almost equally delivered to each cell of all progeny. The self-replication of the SeV vector in infected cells was confirmed by RNA-PCR that amplified the viral RNA genomic sequence (Figure 3a). The GFP cDNA sequence, however, could not be detected by DNA-PCR in the infected cells (Figure 3b), indicating that no DNA phase was involved in the GFP expression.

Pluripotency of infected ES cells

The SeV-infected, fluorescent cynomolgus ES cells were able to form fluorescent tumors when transplanted into immunodeficient mice (Figure 4a–c). The fluorescence was observed uniformly by fluorescent microcopy (Figure 4d and e). The tumors consisted of all three embryonic germ layer cells (Figure 4f–i). Thus, the SeV-infected ES cells were capable of forming teratomas and the SeV infection did not spoil the pluripotency of ES cells. The infected, fluorescent cynomolgus ES cells were also able to generate fluorescent embryoid bodies (Figure 5a and b), MAP-2-positive neurons (Figure 5c), clonogenic hematopoietic colonies (Figure 5d and e), and mature functional (NBT test-positive) neutrophils (Figure 5f and g), all of which fluoresced. In addition, the GFP expression levels were not decreased during the teratoma formation or differentiation, indicating that no 'silencing' of the transgene occurred.

Drug-inducible reduction of transgene expression

Next, we examined whether ribavirin inhibits the replication and transcription of the SeV vector resulting in a reduction of transgene expression. We first used a rhesus monkey kidney cell line (LLC-MK2) to test the effect of ribavirin on the replication and transcription of the SeV vector. LLC-MK2 is a standard control cell line for SeV infection. Ribavirin was added at various concentrations 2 days after the infection. The formation of viral particles quantified by the hemagglutination assay decreased drastically upon the addition of ribavirin (Figure 6a). The decrease was dependent on the dose of ribavirin. The GFP expression was also depressed dose-dependently (Figure 6b). Thus, ribavirin dose-dependently inhibits the replication and transcription of the SeV vector in LLC-MK2 cells. The toxicity associated with ribavirin was not observed in LLC-MK2 cells.

We then examined the effect of ribavirin on SeV-infected, fluorescent cynomolgus ES cells. The addition of ribavirin also resulted in a dose-dependent reduction of GFP expression in the cells (Figure 6c). Although the GFP expression was almost completely inhibited after a 3-day exposure with 4 mM of ribavirin, the cells could not be propagated thereafter. Ribavirin at high concentrations (>1 mM) hampered the proliferation of cynomolgus ES cells. With lower concentrations (0.5–0.75 mM) of ribavirin, the GFP expression level decreased by half. After the discontinuation of ribavirin treatment, the cells could be propagated and nearly regained the original level of GFP expression. The undifferentiated cell fractions were unchanged after the discontinuation as assessed by alkaline phosphatase and SSEA-4 staining (Figure 6d).

Discussion

There are several advantages in using SeV vectors over other vectors. (i) SeV vectors can infect nondividing, quiescent cells as well as dividing cells unlike oncoretroviral vectors.[7–11] Thus, they can be used to infect cells that are terminally differentiated as well as at various stages of differentiation, whether they are dividing or not. (ii) SeV vector-mediated gene transfer does not require a DNA phase. Thus, there is no concern about the unwanted integration of foreign sequences into the host genome unlike with oncoretroviral or lentiviral vectors. (iii) Transgene expression is stable even in dividing cells since the SeV vector replicates by itself in the cytoplasm of host cells. On the other hand, gene transfer using nonreplicating adenoviral and AAV vectors resulted in decreased levels of transgene expression in dividing cells over time, since the non-replicating transgene was